

Permeation Studies of Mixed Matrix Membrane



**By
Sara Abid**

**School of Chemical and Materials Engineering (SCME)
National University of Sciences and Technology (NUST)**

2018

Permeation studies of Mixed Matrix Membrane



Sara Abid

NUST2015-MSCHE00000117496

**This work is submitted as a MS thesis in partial fulfillment of the
requirement for the degree of**

(MS in Chemical Engineering)

Supervisor Name: Dr. Arshad Hussain

**School of Chemical and Materials Engineering (SCME)
National University of Sciences and Technology (NUST)**

February, 2018

Certificate

This is to certify that work in this thesis has been carried out by **Ms. Sara Abid** and completed under my supervision in chemistry laboratory, School of Chemical and Materials Engineering, National University of Sciences and Technology, H-12, Islamabad, Pakistan.

Supervisor: _____

Prof. Dr. Arshad Hussain

Chemical Engineering Department
National University of Sciences and
Technology, Islamabad

Submitted through

Principal/Dean,
Materials Engineering Department
National University of Sciences and Technology, Islamabad

Dedication

To my parents and family

Abstract

Titania nanoparticles have exceptional mechanical properties which make them very attractive for the development of composite membranes. In this research, CO₂, O₂ and N₂ gas permeation behavior of flat sheet composite membranes was examined. The polyamide6 and polysulfone mixed matrix membranes were synthesized using solution casting method. The morphology and dispersion of nanoparticles were observed through SEM. However, the composite membranes were also characterized using several analytical techniques such as universal tensile testing machine (UTM), and thermal gravimetric (TG) analysis. Characterization of these membranes depicted that Titania nanoparticles are extremely compatible with both the polymers. The permeation experiments were performed with CO₂, O₂ and N₂ to explore the host-guest interaction of nanoparticles with chosen gases. The permeability of CO₂ was found pronounced compared to O₂ and N₂ for both polyamide6 and polysulfone MMMs. MMMs with 7wt % Titania loading was found to have higher permeability in case of PA6 and PSf.

Keywords: Nitrogen; polyamide6; polysulfone; oxygen; permeation; MMMs.

Acknowledgments

First of all I would like to thank Almighty Allah who showered His blessings on me and helped me to complete this work. I would also like to express my sincere gratitude to my supervisor Prof. Dr. Arshad Hussain for his guidance, patience and motivation throughout this research work.

I would like to thank my guidance and examination committee members Dr. Abdul Qadir Malik and Dr. Sarah Farrukh for their valuable guidance.

Last but not the least my appreciation also goes to my family and friends for their encouragement, love and support throughout my life.

Contents

Chapter # 1: Introduction	3
1.1. Background	1
1.2. Membrane.....	2
1.3. Modes of membrane processes	3
1.3.1. Dead-end filtration.....	3
1.3.2. Cross-flow filtration	3
1.4. Types of membrane	4
1.4.1. Porous membranes.....	4
1.4.2. Non-Porous membranes	5
Chapter # 2: Literature Review	15
<u>2.1. Membrane gas separation</u>	14
<u>2.2. Materials for membrane gas separation</u>	15
<u>2.3. Mixed matrix membranes</u>	18
Chapter#3: Experimental Methods.....	24
3.1. Materials Used	22
3.2 Membrane Preparation.....	22
3.2.1 Casting Solution Preparation of polyamide6	22
3.3. Gas permeation experiments.....	23
Chapter # 4:Characterization techniques	26
4.1. Scanning Electron Microscopy (SEM)	26
4.1.1. Working Principle.....	26
4.1.2. Information provided by SEM	26
4.1.3. Instrumentation	27
4.2. Thermo gravimetric Analysis (TG)	27
4.2.1 Working Principle.....	28
4.2.2. Types of thermogravimetry.....	28
4.2.3. Instrumentation	28
4.2.4. Applications	29
4.3. Mechanical Testing.....	29
4.3.1. Operation.....	29
4.3.2. Instrumentation	30
Chapter# 5: Results and Discussion.....	34
<u>5.1. Scanning Electron Microscopy Analysis</u>	32
<u>5.2. Mechanical testing</u>	37

__ 5.3. Thermal Gravimetric/Differential Thermal Analysis	41
__ 5.4. Gas permeation results	44
Chapter # 6: Conclusions and Recommendations	55
__ 6.1. Conclusions.....	55
__ 6.2. Future Recommendation.....	56

List of figures

Figure 1.1: Schematic Representation of Membrane Process	3
Figure 1.2: Schematic representation of dead end filtration	5
Figure1.3: Schematic representation of cross flow mode.....	6
Figure1.4: Schematic diagram of types of membranes. a) Isotropic micro porous membrane b) Dense membrane c) Loeb-sourirajan d) Thin-layer Composite membrane .	8
Figure 1.5: Solution casting method	8
Figure 1.6: Symmetric micro porous membranes a. expanded film b.track-etch membranes c. template leaching membranes.....	9
Figure 1.7: Polymer precipitation apparatus	10
Figure 1.8: Schematic diagram of solution-coated composite membranes	10
Figure2.1: Trade-off line curve of oxygen/nitrogen selectivity and oxygen permeability.....	19
Figure 3.1: Schematic representation of permeation testing apparatus.....	26
Figure 3.2: Schematic of Constant Volume Variable Pressure Method.....	27
Figure4.1:SchematicofScanningElectronMicroscope(SEM).....	29
Figure4.2:SchematicDiagramofThermobalance.....	31
Figure 4.3: Tensile Testing Specimen.....	32
Figure 4.4: Schematic Diagram of Tensile Strength Tester	33
Figure 5.1 Surface morphology SEM images of pure PA6 and PA6/TiO ₂ membrane.....	35
Figure 5.2 Cross sectional SEM images of pure PA6 and PA6/TiO ₂ membrane.....	36
Figure 5.3. Surface Morphology of a. Pure Psf b. Psf /2wt%- TiO ₂ c. Psf /5wt%- TiO ₂ d. Psf /7wt%-TiO ₂ e. Psf /10wt%- TiO ₂	37
Figure 5.4. Cross sectional SEM of a. Pure Psf b. Psf /2wt%- TiO ₂ c. Psf /5wt%- TiO ₂ d. Psf /7wt%-TiO ₂ e. Psf /10wt%- TiO ₂	38
Figure 5.5: Tensile strength bar graph of pure PA6 and PA6/TiO ₂ membranes.....	39
Figure 5.6: Tensile strength and % elongation curves as a function of TiO ₂ nanoparticles(wt%)	40
Figure 5.7: Tensile strength bar graph of pure Psf and Psf/TiO ₂ membranes.....	41
Figure 5.8: % elongation curves as a function of TiO ₂ nanoparticles (wt %).....	42
Figure 5.9: TGA curve of pure PA6 membrane.....	43
Figure 5.10: TGA Curves of Various Composite membranes.....	44
Figure 5.11: TGA Curves of Various Composite membranes.....	45
Figure 5.12Trend of permeability with pressure of PA6.....	47
Figure 5.13 TiO ₂ loading ratio vs. permeability of PA6 and PA6/TiO ₂ membranes.....	48
Figure 5.14: Trend of permeability with pressure of Psf.....	49
Figure 5.15: Trend of Permeability of Psf and Psf/TiO ₂ membranes with different TiO ₂ contents.....	50

List of tables

Table 1.1: Illustration of pore size and driving force of different types of microporous membranes 13

Chapter-1

Introduction

This chapter include the over view of membrane technology. Common methods used for the synthesis of nanocomposite membranes are also included in this section. Moreover types of membrane processes and their applications are also highlighted in this chapter.

1.1. Background

The drive towards greater economic and environmental efficiency has resulted in the development of processes with reduced overall environmental impact when compared with existing technology. In the most recent years membranes are picking up a bigger acknowledgment in industry and in the market are contending with conventional operations, for example, pressure swing absorption and cryogenic distillation. Membrane technology are perceived today as effective method in taking care of some imperative worldwide issues, growing new modern procedures required for an economical mechanical development. Energy used for separations consume as much as 40-50% in the current processes, often carried out by ineffective thermally driven separation processes [1].

Membrane technology is now growing gradually. Research work is conducted all over the world in the different subsections of this field. The current research activities are focused on the usage of membranes in different separation techniques on industrial scale. The formation of membranes from different kinds of polymers and their blends are now a days in process. Different processes are used for the separation of gases and other fluids. The main focus is on the separation of CO₂ separation and other gases separation from different processes and the production of membranes for the RO process, biomedical applications and ultra and micro filtrations. In addition to the established membrane

processes new membrane processes such as membrane reactors and contractors are also growing at a rapid rate [1].

In the last few years membrane processes have shown their potential in the advancement of separation processes. Since 1980, a lot of work has been done on it which contributes to the industrial operations such as in refineries and chemical industry. Polymeric Membranes production took the gas separation to the highest level due to reason it does not require phase change like other conventional processes (e.g., cryogenic distillation and adsorption processes), having simplified operation, environmental friendly, flexible operation and good thermal and chemical stability under the wide range of operating conditions.

1.2. Membrane

Membrane is the perm selective barrier between the two phases. It allows one of the components to pass through it which is called permeate and the retaining one is called retentate, making the separation of the mixture possible.

The transport of species through the membrane takes place as a result of driving force between the components in the feed stream. The differential transport occur through various types of driving forces; which may include difference in pressure, temperature difference, electrical potential difference or the concentration difference[3].

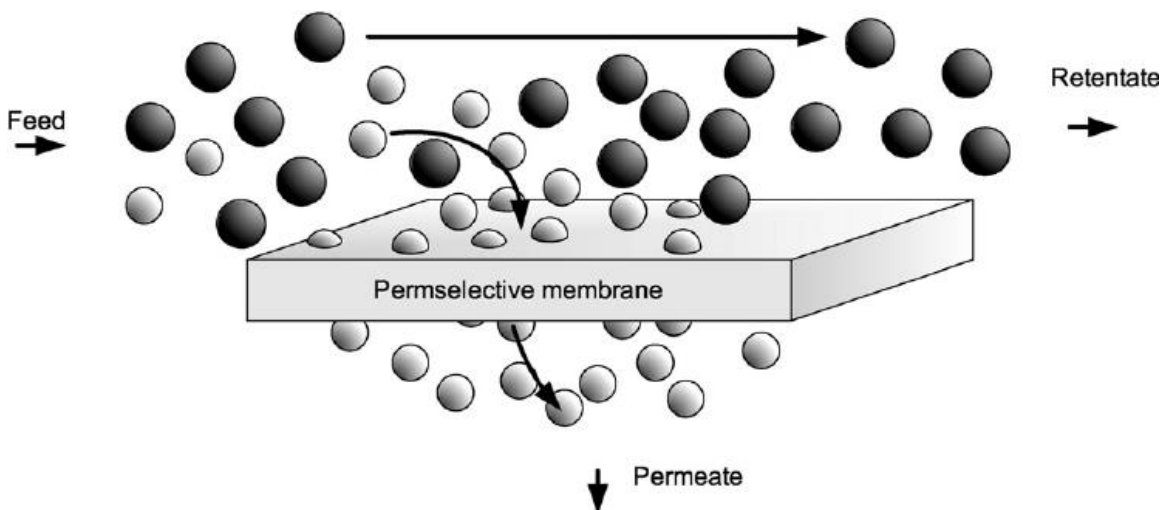


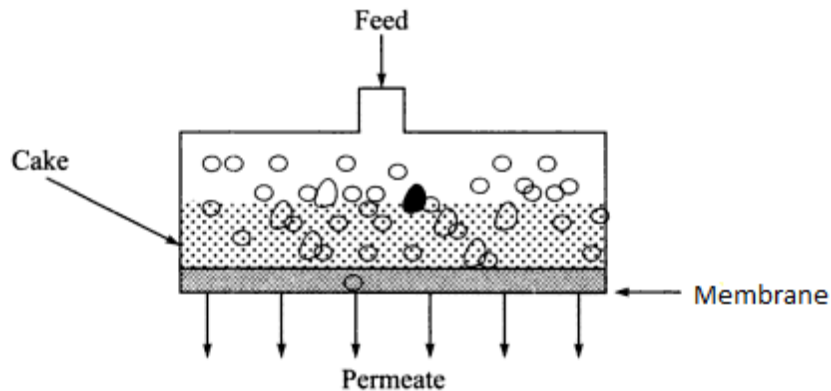
Figure 1-1: Schematic Representation of Membrane Process

1.3. Modes of membrane processes

Direction of flow of feed stream relative to the membrane surface is the main factor which determines the mode of the membranes processes. There are two main modes as follows.

1.3.1. Dead-end filtration

In Dead-end mode, the flow of the feed stream is perpendicular to the membrane surface. The type of flow is suitable for small batch separations as it blocks the



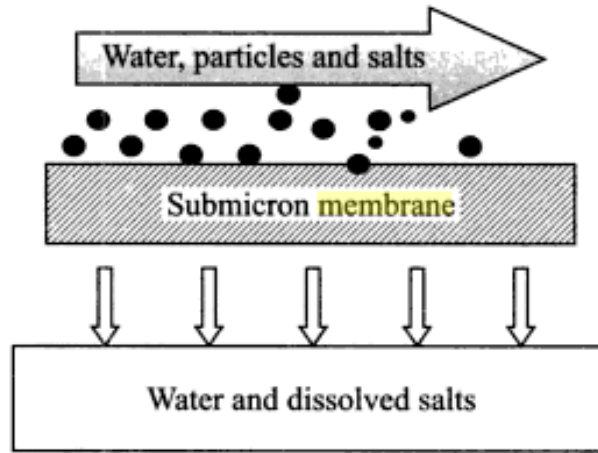
membrane surface by forming cake and is not continuous [7].

Figure 1-2: Schematic representation of dead end filtration

1.3.2. Cross-flow filtration

In cross-flow filtration, the flows of feed stream is parallel to the membrane while permeate flows in a perpendicular direction to the membrane. The flowing feed stream

does
surface
there is
Most



not block the
membrane
as the flow is
parallel and
no cake
formation.
of the
membrane
separation

processes uses cross flow mode [4].

Figure1-3: Schematic representation of cross flow mode[1]

1.4. Types of membrane

Membranes are mainly classified on the basis of flux density and selectivity.

- Porous membranes
- Non-Porous membranes
- Asymmetric membranes

1.4.1. Porous membranes

A porous membrane has a highly voided structure having inter connected pores which are randomly distributed. The separation of the porous membranes depend on the pore size,

pore size distribution and molecular size of the polymer. Chemical and thermal stability also influence the separation. These types of membranes follow pore flow model. Pressure driven flow through these is called convective flow[1].

Micro porous membranes characterized by

- Pore diameter
- Porosity
- Tortuosity

The techniques used to prepare these membranes are

- Sintering
- Stretching
- Phase inversion
- Track –etching

Examples of these membranes are ultra filtration and microfiltration.

1.4.1.1 Micro porous membranes

Micro porous membranes are very similar to the conventional filters in terms of morphology and application. However these pores are very small as compare to the conventional filter (0.01 – 10micron in diameter). Molecular sieving effect is used by the particles which are larger than the size of the pores. These membranes are further classified as

- ***Isotropic membranes:*** Have uniform pore size throughout the membrane
- ***Anisotropic membrane:*** Pore size changes from one surface of the membrane to the other[2].

1.4.2. Non-Porous membranes

Non-porous membranes provide high selectivity for gas separation but the rate of transport is low because of its dense structure. Dense membranes follow solution diffusion method in which solubility and diffusivity play important role [1].

The techniques used to prepare these membranes are

- Melt extrusion
- Solution casting

Dense membranes are used for gas separation and pervaporation.

Based on morphology, there are two types of dense membranes

- Asymmetric membranes
- Composite membranes

1.4.2.1. Asymmetric membrane

Asymmetric membranes are having a thin skin (0.1-1.0 micron) on the surface and the underlying layers are of different material and composition. Porous sub-layer does not have a large effect on the separation properties of the membrane. It only provides the mechanical support. Mass transfer of particular gas through these membranes is dependent on both the thickness and type of material[2].

Asymmetric membranes are further classified as

- ***Integrally skinned***: Here the skin is formed from the phase inversion process
- ***Thin-film composite membranes***: Here the skin layer is homogenous in nature and deposited from solution.

1.4.2.2. Composite membranes

These membranes are referred as second generation membranes. Composite membranes have thin dense polymer on top of the porous substrate. Substrate should be micro-porous so to provide the adequate support to the skin layer. The thickness of the film should be larger than the pores of the substrate. The development of composite membranes has brought a major improvement in RO technology because they have high pH stability and solute rejection[2].

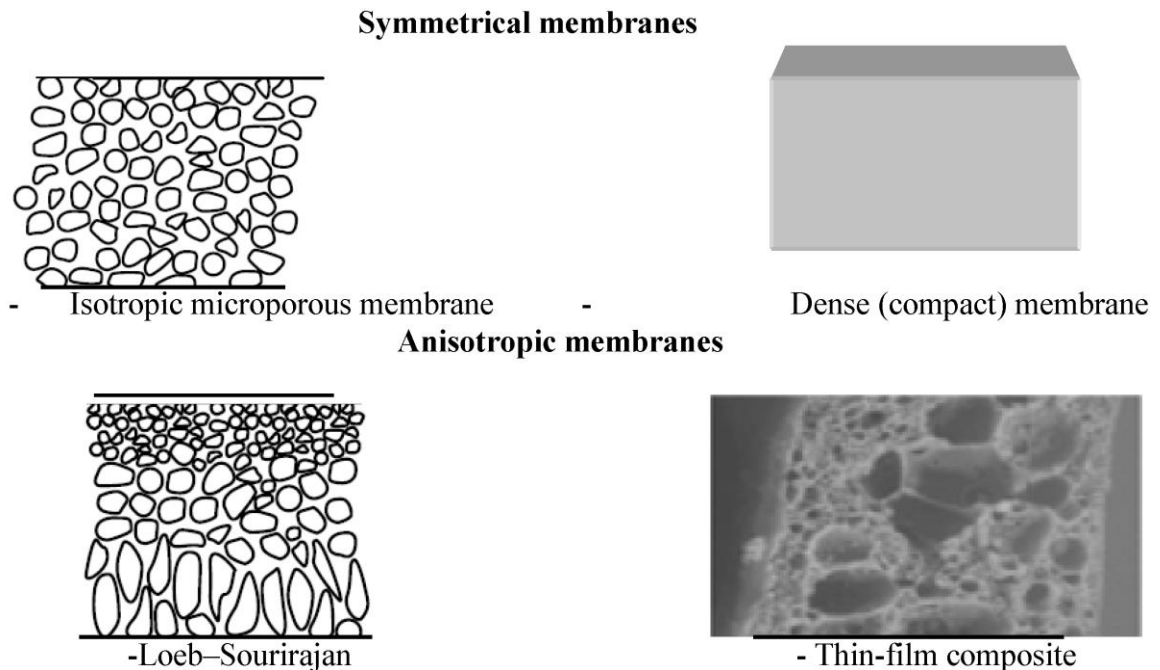


**Figure1-4: Schematic diagram of types of membranes. a) Isotropic micro porous membrane
b) Dense membrane c) Loeb-sourirajan d) Thin-layer Composite membrane**

1.5. Membrane's Casting methods

Various casting methods are used according to the type and application of the membrane. Casting methods are divided on the basis of membrane types.

1.5.1. Symmetric Membranes

- Symmetric nonporous membranes
- Symmetric micro porous membranes

1.5.2. Asymmetric Membranes

- Phase separation membranes
- Solution-coated composite membranes
- Interfacial polymerization membranes

1.5.1.1. Symmetric Non Porous Membranes

Symmetric non porous membranes are widely used in laboratory to measure the membrane properties. These membranes are not used on commercial level as its

transmembrane flux value is too low. Solution casting method is used to produce these membranes.

- **Solution casting method**

An even layer of polymer solution is poured on the surface with the help of casting blade. After casting the solution is left behind to evaporate completely to give a thin and uniform film. This technique is used for small scale experiments.

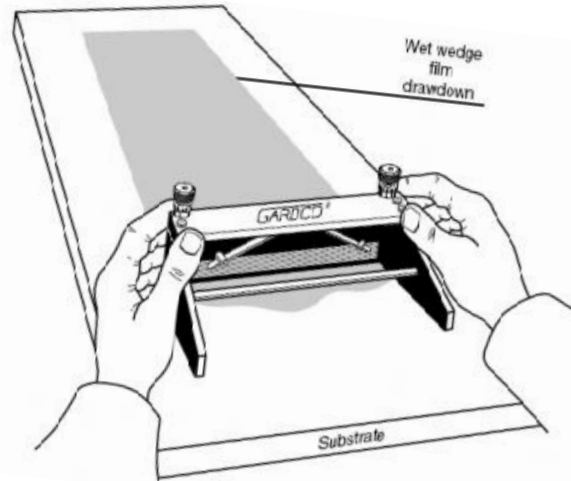


Figure 1-5: Solution casting method

1.5.1.2. Symmetric micro porous membranes

Symmetric micro porous membranes are used for microfiltration membranes because of its higher fluxes than the dense membranes. Its other main application is in the battery and fuel cell as inert spacers. There are three types of symmetric micro porous membranes.

- **Expanded-Film Membranes:** polymer extruding close to its melting point and stretching it to 300% then
- **Template leaching Membranes:** Formation of films using polymer and leachable component which is extruded several times before casting. After formation of films, solvent is used to remove the leachable component.
- **Track-etch Membranes:** Irradiation of fission particles on the polymer film followed by the immersion of this film in the suitable solvent which etches the nucleation tracks forming pores.

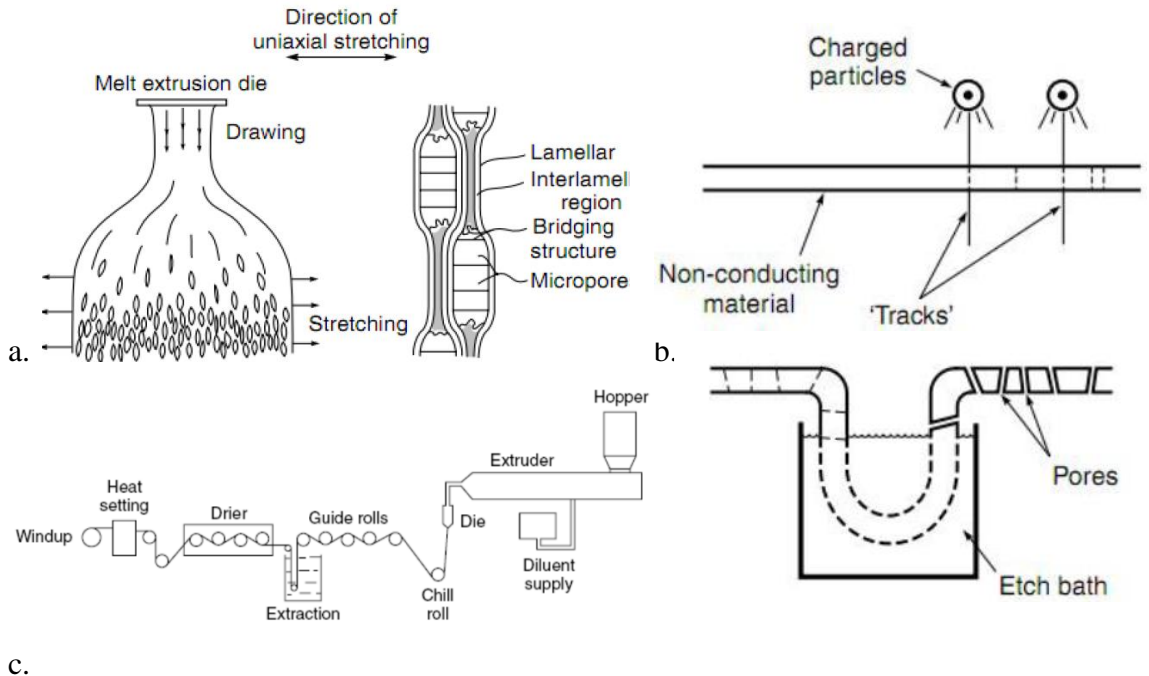


Figure 1-6: Symmetric micro porous membranes a. expanded film b.track-etch membranes c. template leaching membranes

1.5.2..1. Phase separation membranes

These include the precipitation of casting solution in a non solvent bath by immersing it. This technique is also called phase inversion method. In this method, the polymer solution is precipitated into two phase i.e. solid phase-which is polymer rich phase forms the membrane and the liquid phase- which is polymer pore phase forms the pores of the membrane. These can be divided into four ways.

- Precipitation by solvent evaporation
- Precipitation by absorption of water from the vapor phase
- Precipitation by cooling
- Loeb–Sourirajan technique

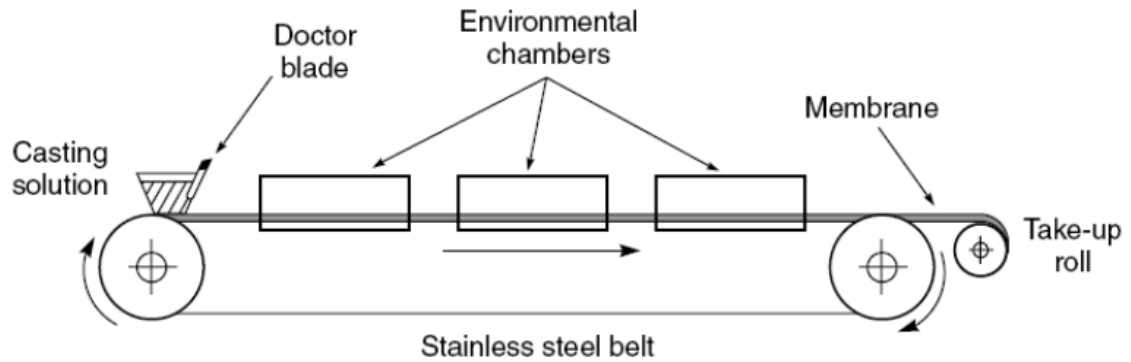


Figure 1-7: Polymer precipitation apparatus

1.5.2.2. Solution-coated composite membranes

One or more dense polymer layer is solution coated on the surface of porous support. A polymer solution is spread over the water bath having a water insoluble solvent. The main problem occurs in transferring the thin film onto the micro porous support.

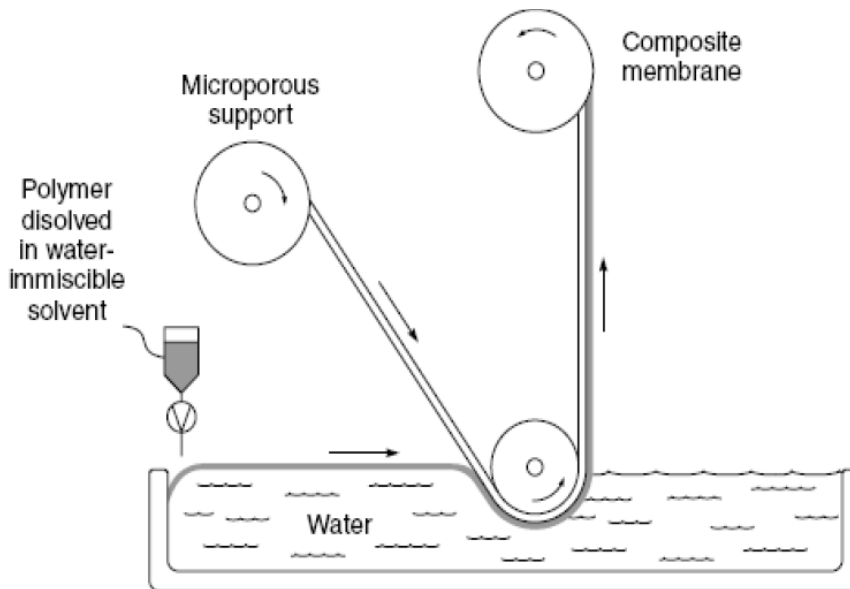


Figure 1-8: Schematic diagram of solution-coated composite membranes

1.5.2.3. Interfacial polymerization membranes

This is the most important technique of all the casting methods. This method is mainly used for gas separation, reverse osmosis and ultrafiltration. This kind of Membranes consists of dense top Layer on the surface of micro porous support.

1.6. Applications of membrane processes

1.6.1. Microfiltration (MF)

Microfiltration is widely used for higher than 0.08-2 μm and operates within a pressure range of 5-100 kPa to remove colloidal and suspended particles. It is used to separate particulate matter, colloids from the solution and bacteria. Pore size of microfiltration membrane is in the range of 0.1 to 10 micron. [5].

Industrial applications include

- Waste water treatment
- Clarification of fruit juice, wine and beer
- Production of ultra-pure water for semi-conductor industry
- Metal recovery as colloidal oxides or hydroxide
- Separation of oil water emulsions

1.6.2. Ultrafiltration (UF)

Pore size of ultrafiltration membranes is in the range of 0.05 micron to 1 nanometer. It is most commonly used for the separation of macromolecules, colloids from the solution, recover oils and to produce ultra pure water. The ultrafiltration process lies between the nanofiltration and microfiltration. It is a pressure driven membrane process which operates in the range of 70-700kPa[5].Common applications are removal of proteins and carbohydrates, to remove viruses and endotoxins and removal and recovery of oils, surfactants and paints from waste streams

1.6.3. Reverse osmosis (RO)

Reverse osmosis is commonly used for the separation of dissolved ions from water. Particles greater than 0.001 microns are rejected and retained on the surface of membrane. It is a pressure driven process which operates within a range of 2 to 10 MPa[5].Industrial applications are production of portable water by desalination of

brackish and seawater, to produce ultrapure water in the semiconductor industry and reverse osmosis membranes are used to purify rain water for landscape irrigation

1.6.4. Nanofiltration(NF)

Nanofiltration membranes are intermediate between the reverse osmosis membranes and Ultrafiltration membranes. They have lower salt rejection but higher permeability of water as compare to RO membranes. These membranes are also known as “loose reverse osmosis”. Pore size of nanofiltration membranes is within the range of 1-10 nanometers. Applications include water softening, Removal of contaminants from water and acid stream and water purity system [4].

1.6.5. Gas separation(GS)

Gas separation is the process in which gas mixture at high pressure is passed through a dense membrane which allows one of the components of the mixture to pass through it readily. The driving force is the concentration difference or the hydrostatic pressure difference[4].Common applications include Hydrogen separation and recovery, CO₂ enhanced oil recovery, Natural gas processing and Air separation

Sr. #	Membrane Process	Pore size of membrane	Driving force
1	Microfiltration	Symmetric microporous, 100-10000nm	Hydrostatic pressure difference (10-500 kPa)

2	Ultrafiltration	Asymmetric microporous, 1-10nm	Hydrostatic pressure difference (0.1-1 MPa)
3	Nanofiltration	Thin film membranes, order of nm	Hydrostatic pressure difference (9.3-15.9 bar)
4	Reverse Osmosis	Asymmetric skin-type, 0.5- 1.5nm	Hydrostatic pressure difference (2-10MPa)
5	Gas separation	Non porous (or porous < 1nm)	Hydrostatic pressure and concentration gradient

Table1.1: Illustration of pore size and driving force of different types of microporous membranes

Chapter-2

Literature Review

This chapter comprises of summary of the research work already carried out on the nanocomposite membranes for gas separation applications. Different materials used for gas separation applications have also been discussed.

2.1. Membrane gas separation

Membrane gas separation has a broad range of industrial applications in refineries and chemical industries. Till the record membrane gas separation processes has acquired more importance as the unit operation method over the GS processes like adsorption, absorption and cryogenic distillation. It is because of the fact that membrane gas separation does not require any phase change and low energy cost. Moreover this process is best suited for use in remote areas because of its easy and simple process and compact equipment. Baker estimated that the expansion of membrane gas separation in coming years will be increased from today[6]. It is predictable that membrane technology will play a significant role in dropping the ecological pollution and the cost of conventional separation processes[7].

Membrane separation process became economically competitive in 1970s [12] and since then it has always been more attractive than conventional processes. Gas separation (G S) among other types of separations is gaining importance day by day. Since 1980, a lot of work has been done on it which contributes to the industrial operations such as in refineries and chemical industry. Polymeric membranes production took the gas separation to the highest level due to reason it does not require phase change like other conventional processes (e.g., cryogenic distillation and adsorption processes)[8].

For this process to be more effective, fabrication of efficient membranes is the most important factor. Two main parameters which are important for membrane process are permeability and selectivity. Gas separation using polymeric membranes is considered as the most feasible technique due to easy scale up and least requirements in terms of energy, maintenance and cost [11].

Now days, membranes have been used in numeral GS applications such as, air separation, hydrocarbons purification, natural gas and flue gas purification. Research has been done on the different polymers for gas separation to study the permeation of oxygen, nitrogen

and carbon dioxide. However, there has been no work done on the aliphatic polyamides in the area of gas separation. This field needs special attention as a membrane for GS as it's being used as a part of composite membranes which is reported in the different research papers.

Many opportunities are there to widen the scope for gas separation membranes. To exploit these, current membrane materials and membrane preparation routes are not enough. A wide range of materials were tested in this area. A large amount of the research work is focused now a days to investigate new membrane materials and to develop new membrane modes that results in better selectivity and permeability for gases like carbon dioxide, nitrogen and oxygen [9].

2.2. Materials for membrane gas separation

For the selection of membrane material, the physical and chemical properties are considered as these properties accounts for the advancement in the process. In addition to this, more stable and strong materials are required for Gas separation membranes. The properties which matter includes material, membrane structure and thickness and its modes like flat, hollow fiber [8].

Selectivity and permeability plays significant function in the economics of gas separation. Permeability is defined as the rate at which specific compound from the gas mixture permeates through the membrane, which depends upon the kinetic and thermodynamic factors. Selectivity is the relative permeability of the membrane for the feed stream. In history diverse materials have been studied to attain the requisite separation [11]. Amongst all, polymeric membranes stood first in a wide array of industrial applications[12].

Polymeric membranes have exceptional advantages i.e. superior thermal and mechanical properties, low cost, eco friendly and simple process [13- 14].The structure of polymeric chains significantly influenced the gas transport through the membrane. Glassy materials have high mechanical stability and high selectivity as compare to rubbery materials. Because of this glassy polymer are used in commercial GS processes[8].

In last few years a lot of polymeric materials have been studied for GS applications but the polymers used industrially are still in lesser number [15]. Glassy polymers used commercially for membrane gas separation are

- Polyimide
- Polysulfone
- Polycarbonate
- Cellulose acetate
- Polyamide

The selection of polymers or their blends used for membrane separation processes depends on the permeability, selectivity, cost, durability, ease of synthesis and fabrication. Different polymers have been used to study the permeability of various gases. Polyimide is one of the best polymers for the study of permeation. Kusakabe et al. [28] studied polyimide/SiO₂ composite membrane for CO₂ permeability and reported that the permeability was 15 times larger than that in the pure polyimide. Moaddeb and Koros [22] reported that the gas permeation properties of thin polyimide membranes/silica particles have shown enhancement for O₂ and N₂. Due to silica disorderly the polymer chain packing results in the rise in permeability.

Research has been done on the aromatic polyamides for gas separation to study the permeation of oxygen, nitrogen and carbon dioxide. Aromatic polyamides have been used as gas separation membranes in which different monomers were used as substituents. The resulting polyamides had improved properties such as solubility, elevated glass transition temperatures and outstanding mechanical properties. The permeability was found using helium, oxygen, nitrogen, carbon dioxide and methane. Gas permeability was directly related to free volume which was directly proportional to chemical structure.

The experimental aromatic polyamides described a favorable blend of permeability–selectivity, better than that of conventional polyamides confirming the theory that the inclusion of side bulky substituents is a suitable approach to hold back the inherently efficient chain packing of polyamides [27]. Cardo polyamide membranes have been used for hollow fiber membranes showing the permeability of O₂ and N₂ increased with the increase in temperature, showing 20 times higher rate at 240°C [1].

The gas permeability of amorphous polymers has a strong relationship among the structure and its properties of a polymer as a membrane for gas separation. Advancement of the chemical structure of a polymer chain direct to improved permeability coefficient and selectivity or vice versa [2].

The asymmetric aromatic polyamide membranes coated with silicone rubber were used for investigating the permeation rate for O₂, N₂, CO₂, and He & CH₄. Membranes were made by phase inversion method showing the increase in permeability with the increase in pressure. The comparison of permeability in coated and uncoated membranes showed that the permeability is less in coated membranes compared to the other[5]. However, there has been no work done on the aliphatic polyamides in the field of gas separation to study the permeation of different gases like CO₂, N₂ and O₂.

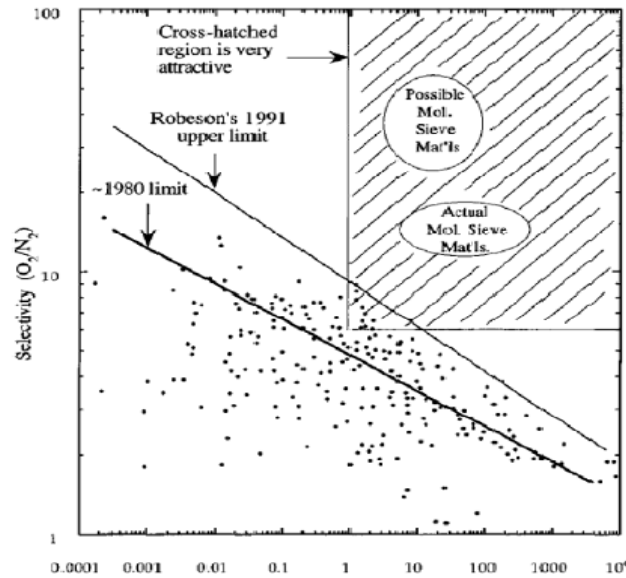


Figure2.1: Trade-off line curve of oxygen/nitrogen selectivity and O₂ permeability [6]

Work has already been done in order to advance the performance of membranes which includes a major work by Robeson who investigated the properties of different polymers [13]. The polymeric membranes have opposite correlation between selectivity and

permeability. Selectivity decreases with increase in permeability or vice versa. Figure 2.1 shows the line curve of oxygen/nitrogen selectivity and oxygen permeability. It clearly indicates the inverse relation between selectivity and permeability.

Polysulfone (PSU) is a type of thermoplastic extensively used in the membranes. It was used as substitute for polycarbonates owing to the elevated mechanical strength in nature by Union Carbide in 1965 [25]. Monsanto Co. introduced polysulfone as the first polymeric material used in the wide scale membrane gas separation in 1970s [45].

As illustrated in the Robeson upper bound, PSU reported as a subordinate candidate in terms of permeability and selectivity compared to others. However, it still have high potential to be commercially practical membrane due to its high strength and dimensional stability [26].

Genne et al. reported that the permeability of membranes increases by increasing the weight fraction of ZrO_2 nanoparticles in polysulfone membranes[20]. Kiadehi et al, studied Novel carbon nano-fibers and polysulfone (PSf) membranes for gas separation and reported 2.2 barrer anpermeability of O_2 [19].

2.3. Mixed matrix membranes

Polymeric membranes are still an excellent candidate for gas separation despite of the limitation in robenson curve. To beat this drawback, modification in the polymers has done by means of the mixture of polymeric and inorganic material recognized as mixed matrix membranes [16]. Mixed matrix membranes (MMMs) is the term used for the membranes in which fillers are incorporated. If the fillers are inorganic nanofillers then the membranes are termed as composite membranes. Composite membranes illustrate elevated gas permeabilities than pure polymer membranes. For example the addition of inorganic functional groups on inorganic fillers results in enhanced selectivity and permeability. Structure of the membranes can be controlled by the type of bonds between organic and inorganic phases[17].

An significant contribution in the gas separation field is the use of inorganic fillers in the polymers to enhance the permeation and its other properties. A large number of fillers are used among which the widely used are CNT's, SiO_2 , TiO_2 , zeolites and carbon nanotubes. Mixed matrix membranes (MMMs) is the term used for the membranes in

which fillers are incorporated. This field has gained importance in the last few years due to its better results in the separation of gas and liquid and its other properties (mechanical, thermal). Among the list of fillers, TiO_2 has gained importance due to its availability and other properties like low cost, high stability and environmental friendly.

Titania nanoparticles have been used in two forms in the membranes either in the membrane matrix or on the surface of the membrane through coating method. P. safaei et al.[6] Studied the effect of TiO_2 in the polystyrene that revealed 7wt% TiO_2 gives best results for the permeation study of CO_2 . In another study, the effect of Titania nanoparticles with PSF was studied in which the CO_2 and CH_4 permeance decreases in low wt% of TiO_2 and increases in high wt% of TiO_2 [7]. PVA/ TiO_2 nanocomposite membranes were prepared by Jamil Ahmed et al.[8] to study the gas permeation properties for the gas pairs O_2/N_2 , H_2/N_2 , and CO_2/H_2 , showing at low loading of TiO_2 the permeability decreases.

Hu et al. [9]studied Fluorinated polyamide- imide/ TiO_2 nanocomposite membrane which showed higher permselectivity for CO_2 at low loading of TiO_2 . Matrimid-5218/ TiO_2 based MMMs were also studied by Moghadam et al. [10]to study the effect of filler which showed the gas permeability increases with high loading of TiO_2 . Also the effect of nanoparticles was studied by Kong et al. [11] in which they study the effect of TiO_2 with polyimide membranes. Their results showed that with 25wt% TiO_2 , the permeability of gases (N_2 , H_2) is increased.

Solution blending is a very simple approach to synthesize mixed matrix membrane. In this technique the polymer is first dissolved in a suitable solvent. Then the nanoparticles are mixed with the prepared solution. The mixture is then stirred to disperse the added inorganic nanoparticles. The composite membrane is then casted by removing the solvent by traditional means [19]

I.Genne et al. fabricated polysulfone zirconia oxide nanocomposite membranes by using polymer solution containing 18 wt % of polysulfone dissolved in methylpyrrolidone. Various amounts of ZrO_2 nanoparticles are added in the polymer solution.Genne et al. showed that the permeability of membranes increases by increasing the weight fraction of ZrO_2 nanoparticles[20].

S. Farrukh et al. [11] studied the effect of TiO₂ nanoparticles on gas permeation and CO₂ permeability was enhanced due to the interaction between CO₂ and TiO₂ nanoparticles. Ahmed et al. reported the mechanical, chemical properties of PVA/ titanium oxide composite membranes made by solution blending method. Membrane selectivity was increased for the oxygen/nitrogen, hydrogen nitrogen and carbon dioxide/ nitrogen gas pairs up to 60%, 55% and 26% respectively by the addition of titanium oxide nanoparticles with subsequent decrease in the gas permeability. Reverse trend was observed at higher loading of TiO₂ nanoparticles.

Liu et al. fabricated polymethacrylic acid/ titanium oxide mixed matrix membranes by using nanoparticles of titanium oxide enwrapped with organic membrane by microwave induced plasma method[24]. Kusakabe et al. synthesized polyimide/ SiO₂ nanocomposite membranes. The gas permeation results showed that the permeability of carbon dioxide was 15 times greater in the prepared hybrid nanocomposite membranes as compared to pure polyimide membranes [38].

Smaihi et al. prepared polyimide siloxane nanocomposite membranes containing various weight fractions of silica by sol-gel method. Two different coupling agents were used i.e. aminopropyltrimethoxysilane (APrTMOS) and aminopropylmethyldiethoxysilane (APrMDEOS). Lower gas permeability was observed by using APrTMOS as a coupling agent compared to APrMDEOS at same silica weight fraction. [39]. The prepared membranes were tested for carbon dioxide, hydrogen and nitrogen gas. The permeation testing showed that the membranes had higher permeability of carbon dioxide ($P_{CO_2} = 41$) compared to hydrogen ($P_{H_2} = 10.3$ Barrer) and nitrogen ($P_{N_2} = 7.74$ Barrer) [40].

Moaddeb et al. fabricated polyimide/silica nanocomposite membranes to study the gas permeation properties of polyimide membranes in the presence of nanoparticles of silica. The presence of silica nanoparticles enhanced the gas permeability of the polyimide mainly for oxygen and nitrogen. The author attributed the increased permeability of prepared nanocomposite membranes to the disruption of polymer chains packing due to the presence of silica nanoparticles. [41].

Hibshaman and coworkers reported the assembly of polyimide/silica composite membranes. They observed the effect of loading of alkoxysilanes on the permeability and selectivity of various gases including carbon dioxide, nitrogen and methane. The

membranes were prepared from hexafluoroisopropylidenediphthalic anhydride, diaminobenzoic acid, phenyltrimethoxysilane and TMOS.. Best results were obtained with 22.5 wt% of TMOS. By using 22.5 wt % of TMOS the permeability of carbon dioxide was 80 Barrer[42].

Suzuki et al. studied the physical and gas transportation properties of hexafluoroisopropylidenediphthalic anhydride (6FDA) based polyimide/silica nanocomposite membranes. The membranes were prepared by using polyamic acid, TMOS and water. Sol-gel method was used for membrane preparation. Results revealed that the permeability of carbon dioxide, oxygen and nitrogen was increased by increasing weight fraction of silica nanoparticles. The author attributed the increased gas permeabilities to the improved solubilities of gases in the membranes. Results revealed that the prepared membranes had elevated gas selectivity and excellent thermal stability and are therefore predicted to be very good gas separation membranes[43].

Poly (amide-6-b-ethylene oxide)/silica nanocomposite membranes were fabricated by Kim and coworkers by in situ polymerization of tetraethoxysilane (TEOS). Permeation tests were performed for various gases including carbon dioxide, nitrogen and oxygen. Results declared that the permeability and selectivity of the nanocomposite membranes were higher than those of pure Poly (amide-6-b-ethylene oxide). Highest permeability was observed with carbon dioxide at 27 wt. % silica. At this silica content, the permeability of carbon dioxide was 277 Barrer[44].

Chapter-3

Experimental Methods

This chapter includes materials and methodology adopted for the synthesis of (polyamide6, polysulfone)/TiO₂ nanocomposite membranes.

3.1. Materials Used

- Polyamide6 (Nylon6) were purchased from Sigma Aldrich
- polysulfone
- Titanium dioxide (particle size of 21 nm and specific surface of around 50 m²/g) were supplied by Sigma Aldrich.
- Formic Acid (Purity >98%)
- Chloroform
- Nitrogen, Oxygen and Carbon dioxide gas (purity 99.5%)

3.2. Membrane Preparation

Synthesis of polyamide6/TiO₂ and polysulfone/TiO₂ nano composite membranes involved the following steps.

3.2.1 Casting Solution Preparation of polyamide6

PA6/FA/TiO₂ flat sheet membranes were prepared by solution casting method. The polyamide solution was dissolved in 8ml formic acid in air sealed bottles. This solution was stirred by using a magnetic stirrer at room temperature for 24 hours. Solution was prepared for pure membrane and for different wt% of TiO₂ nanoparticles in different air sealed glass bottles. Different weight fractions of titania nano particles were dissolved in half of the amount of the solvent of formic acid in different viels and was stirred at room temperature for 24 hrs using magnetic stirrer to get a homogenized mixture. After stirring the solution was sonicated with the help of probe sonicator for almost 2-3 hrs to break the accumulation of nano particles. Then this solution was mixed with the pre-stirred solution of PA6/FA at room temperature and was stirred for again 24hrs. After this the resulting solution was sonicated again for 2hrs at room temperature to well disperse the TiO₂ particles in PA6 solution.

- **Membrane Casting and Drying**

In the next stage, pour the solution in the Petri dish to make thin films. This Petri dish was then placed in the vacuum oven at 75°C and dried to remove the moisture and remaining solvent for 2hrs.

3.2.2. Casting Solution Preparation of polysulfone

Solution casting method was used to prepare Psf/CF/TiO₂ flat sheet membranes. 0.518g of polysulfone was dissolved in 10ml chloroform in an air tight bottle. This solution was allowed to stirring for about 2 hrs by using mechanical stirrer. Solution was prepared for pure polymer membrane and for different wt% of TiO₂ nanoparticles in different air sealed glass bottles. Different weight fractions of titania nano particles were dissolved in half of the amount of the solvent of chloroform in different viels and was stirred at room temperature for 2hrs with the help of magnetic stirrer to get a homogenized mixture. Then this solution was sonicated with the help of probe sonicator for 30 minutes to disperse the nanoparticles. After that the half of the polymer solution is poured in this solution and leave for stirring for about 1 hr. Then this solution is again sonicated for 30 mints and the remaining polymer solution is added in it and then again it is stirred and sonicated in the same manner as above.

- **Membrane Casting and Drying**

In the next stage, pour the solution in the petri dish to make thin films. This solution is allowed to dry in the room temperature for 24 hrs with the lid on the petri dish. After 24 hrs, remove the lid of the petri dish and leave for drying again for 24 hrs. on the next day place this petri dish in the oven at 85°C and allowed to dry to remove the remaining solvent.

3.3. Gas permeation testing

Gas permeation testing were performed by using apparatus shown in Figure 3.1, which includes

- flow meters (1)
- gas cylinder (2)
- Pressure regulators (3)
- membrane module (4)
- pressure sensor (5)

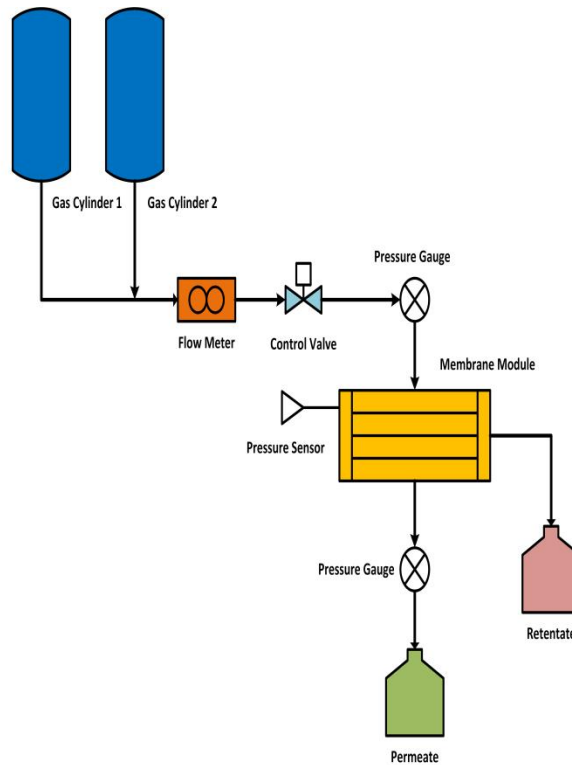


Figure 3.1: graphic diagram of permeation testing apparatus

The gas permeability test system (PHILOS, Korea) was used to measure the permeability of the gases i.e. carbon dioxide, oxygen and nitrogen. Mass flow controllers control and detect the feed and permeate flow rates in order to keep the flow rate and pressure within allowable limits while back pressure valve is used to maintain a given differential pressure across the membrane. Flow and pressure indicators display gas flow and pressure on feed, concentrate and permeate side. Gases are provided from cylinders to feed side and membranes are tested at constant volume and variable pressures from 2 to 4 bar. A certain pressure difference is maintained across the membrane to determine the flux through membranes. This system contains porous ceramic support with effective area of 8.5cm^2 . A bubble flow meter is also utilized to determine the flow rates below 10 ml/s. The permeability test system provides us with very accurate values for pressure and flow rate which are used to determine the permeability.

Solution diffusion model was used to calculate the Permeability of gases [56] as follows

$$P = \frac{Q * L}{\Delta P * A}$$

Q = Volumetric flow rate (ml/min)

A = effective membrane area (m²)

L = Membrane Thickness (m)

ΔP = Pressure difference (bar)

Chapter-4

Characterization Techniques

This chapter highlights the means and ways adopted for the characterization of fabricated membranes. It also includes the brief description of the techniques used for the characterization of fabricated membranes.

Characterization techniques

4.1. Scanning Electron Microscopy (SEM)

Scanning electron microscope is most commonly used electron microscope. It examines the microscopic structure of the materials by focusing a beam of high energy electrons on the materials surface. The electron beam generates a variety of signals at the surface of the material, which provides the information about the morphology (texture) and chemical composition of the sample. In most cases information is collected over the chosen area of the sample surface. Analysis of selected points on the sample surface can also be performed by SEM. The function of SEM is very similar to the electron probe microscope.

4.1.1. Working Principle

The high energy beam of electron is focused on the solid surface of the sample. The kinetic energy of the electrons is dissipated as a variety of signals as these electrons are decelerated in sample. Sample image is mainly formed by secondary electrons and backscattered electrons. Backscattered electrons are more valuable in phase discrimination and secondary electrons are more important for viewing the morphology and topography of the sample. X-rays are produced by the collision of incident electrons and the electrons present in the shells of the sample atoms. The yield x-rays have fixed wavelength and are produced for each element in a mineral that is excited by the high energy beam of electron. SEM is non destructive technique as the electron interactions do not lead to the volume loss of the sample.

4.1.2. Information provided by SEM

SEM analysis provides the following information about the sample

- Morphology: related to the size and appearance

- Topography: related to the surface characteristics of the sample
- Crystallography: Shows how atoms are arranged in the sample

4.1.3. Instrumentation

- Electron gun
- Electron lenses
- Sample stage
- Detector
- Data output devices

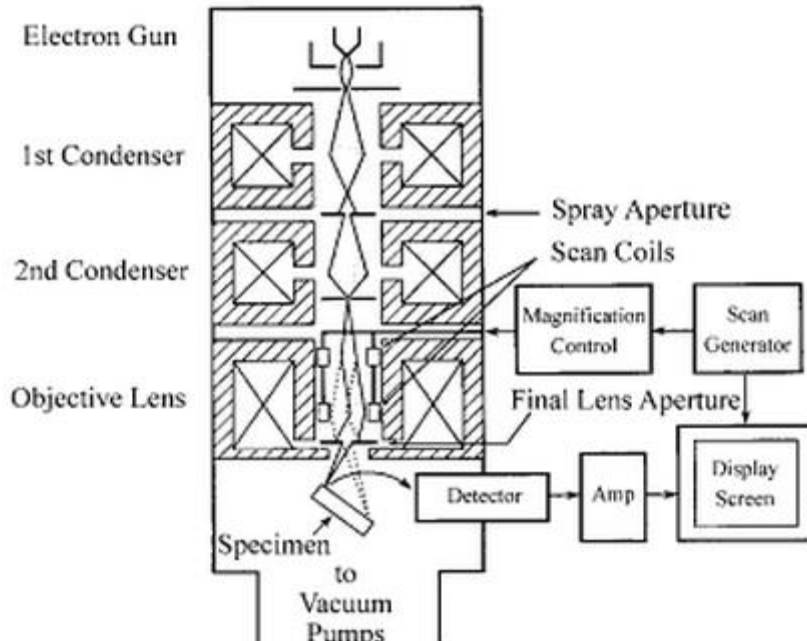


Figure 4.1: Schematic of Scanning Electron Microscope (SEM)[44]

4.2. Thermo gravimetric Analysis (TG)

Thermogravimetry analysis is an analytical technique used to determine the weight change of a sample either as a function of time isothermally or as a function of temperature in an inert atmosphere of nitrogen, helium or in vacuum. Inorganic materials, metals, polymers and composite can be analyzed with the help of TGA. Sometimes the measurement is carried out in a lean oxygen atmosphere to slow down oxidation. [31]

4.2.1 Working Principle

Thermogravimetry analyzer consists of a sample pan in which sample is placed. That pan is supported in a furnace and is heated at constant heating rate during the experiment. Weight change of a sample is recorded during the experiment. Sample environment is controlled by purge gas. In most of the cases purge gas is air, helium, nitrogen or argon. Thermal events like absorption, desorption, sublimation, oxidation and decomposition bring a severe change in mass of the sample. Hence TGA is used to determine the kinetics and thermal stability of the materials. [32]

4.2.2. Types of thermogravimetry

There are three types of thermogravimetry

Isothermal TGA: Sample is analyzed at constant temperature for fixed period of time and weight change of the sample is recorded w.r.t time

Dynamic TGA: Sample is heated at constant heating rate and weight change is recorded as a function of temperature

Quasistatic TGA: Sample is heated to a constant rate at series of increasing temperature [33]

4.2.3. Instrumentation

Thermogravimetry analyzer mainly consists of

- Electronic microbalance
- Furnace
- Temperature programmer and recorder

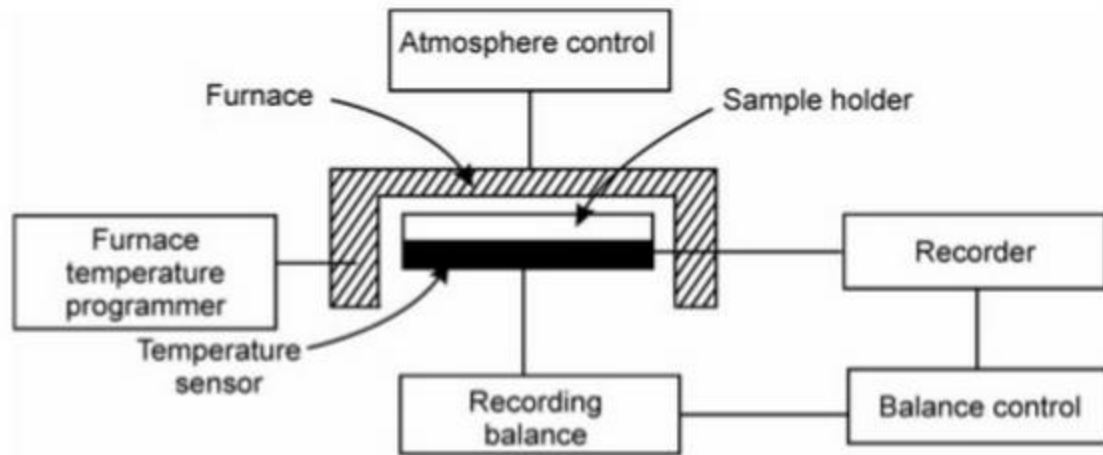


Figure 4.2: Schematic Diagram of Thermobalance [31]

4.2.4. Applications

Common applications includes

- Thermal stability
- Kinetic studies
- Material characterization
- Compositional analysis

4.3. Mechanical Testing

Tensile testing is also known as tension testing. It is a fundamental test in which the sample is subjected to a controlled stress until failure. It is used to predict the behavior of the sample under loading. It is commonly used to determine the maximum stress that a material can withstand without failure. Ultimate tensile strength and maximum elongation are directly measured with the help of tensile test. With the help of these measurements young's modulus, yield strength and strain hardening characteristics of the sample can be determined [46]

4.3.1. Operation

An axial force is applied on the sample of original length L_0 to elongate it. Due to elongation the cross sectional area of the sample is reduced to A from A_0 until fracture. The change in length and load between the gauge length is recorded to measure the stress strain relationship

4.3.2. Instrumentation

- Load cell
- Moving cross head
- Fixed cross head
- Base and actuator

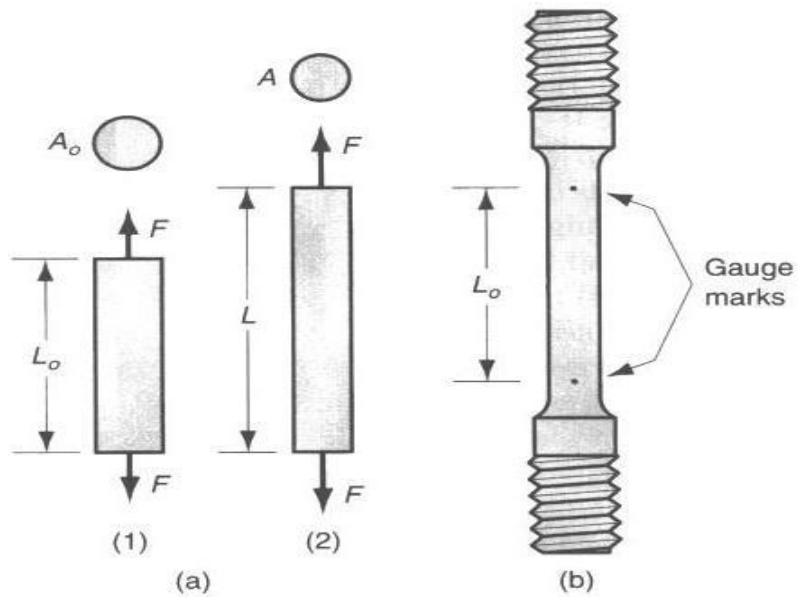


Figure 4.3: Tensile Testing Specimen [33]

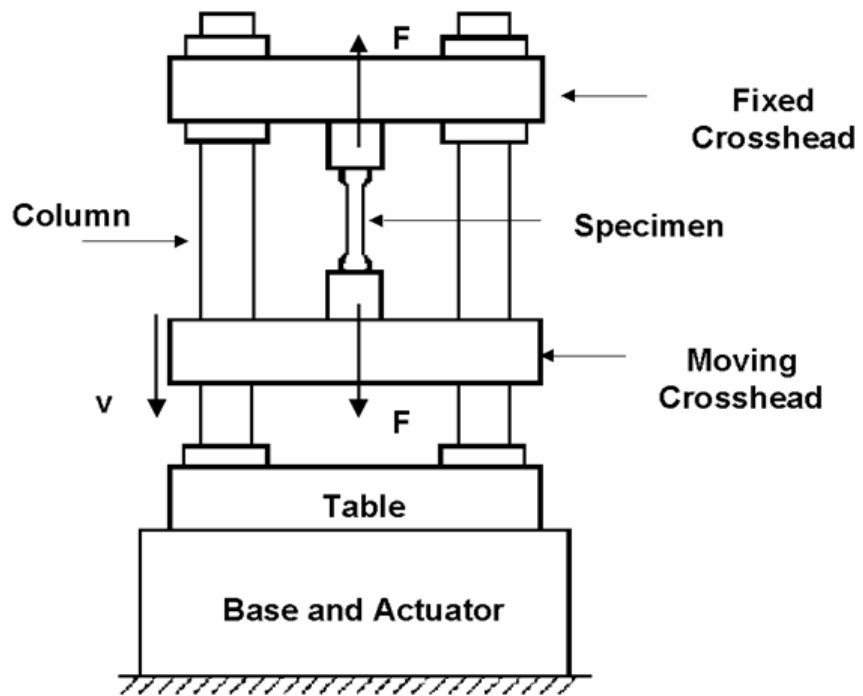


Figure 4.4: Schematic Diagram of Tensile Strength Tester [33]

Chapter-5

Results and Discussion

Part of this chapter deals with the characterization of fabricated membranes. Results obtained as a result of characterization are discussed in detail. Second part of this chapter includes the gas permeation study of fabricated membranes. Effect of feed pressure and TiO₂ loading ratio on gas permeabilities are discussed in detail.

5.1. Scanning Electron Microscopy Analysis

The surface study of the PA6 and PA6/TiO₂ was analyzed by scanning electron microscopy. The Figure 5.1 depicts the morphology of the fabricated membranes having different wt% of Titania particles at $\times 10,000$ magnification. The surface of the pure membrane shows that it is highly dense and non porous having smooth surface. However, the surface of the blended membranes shows smooth surface showing the homogenous blending of the nanoparticles in the polymer matrix. The Polyamide6 forms weak complexes with the formic acid after dissolving; when the solvent evaporates it breaks the weak interaction between the complexes leaving behind the surface smooth as shown in the figure2. If the solvent do not evaporate completely it would have appear as a small tiny particle on the surface [34]. SEM image of the fabricated membranes confirms the homogenous blending and bonding between the nanoparticles and the polymer.

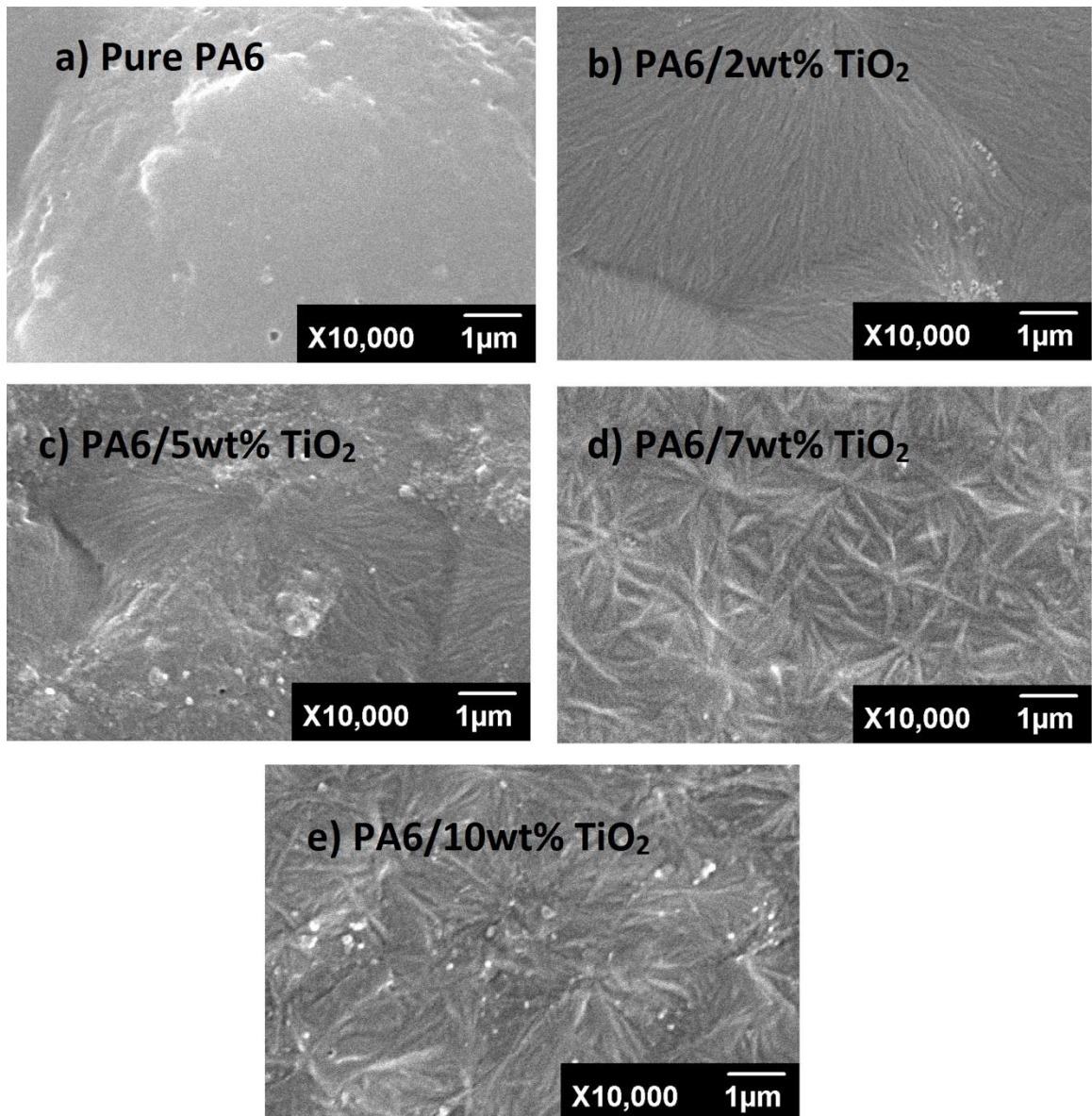


Figure 5.1 Surface Morphology of a. Pure PA6 b. PA6/2wt%- TiO₂ c. PA6/5wt%-TiO₂ d. PA6/7wt%- TiO₂ e. PA6/10wt%-TiO₂

Figure 5.2 shows the cross-sectional area of the fabricated membranes i.e. pure PA6 and PA6/TiO₂ which shows the membranes are dense. However, there are void generations in the sub layer of the membranes indicating the increase in the free volume. The reason behind is the interactions of the Titania with polymer chains, which disturb the polymer chains resulting in the disorder of the packing and the gathering of Titania particles. These are the factors which may contribute to the higher value of the permeability.

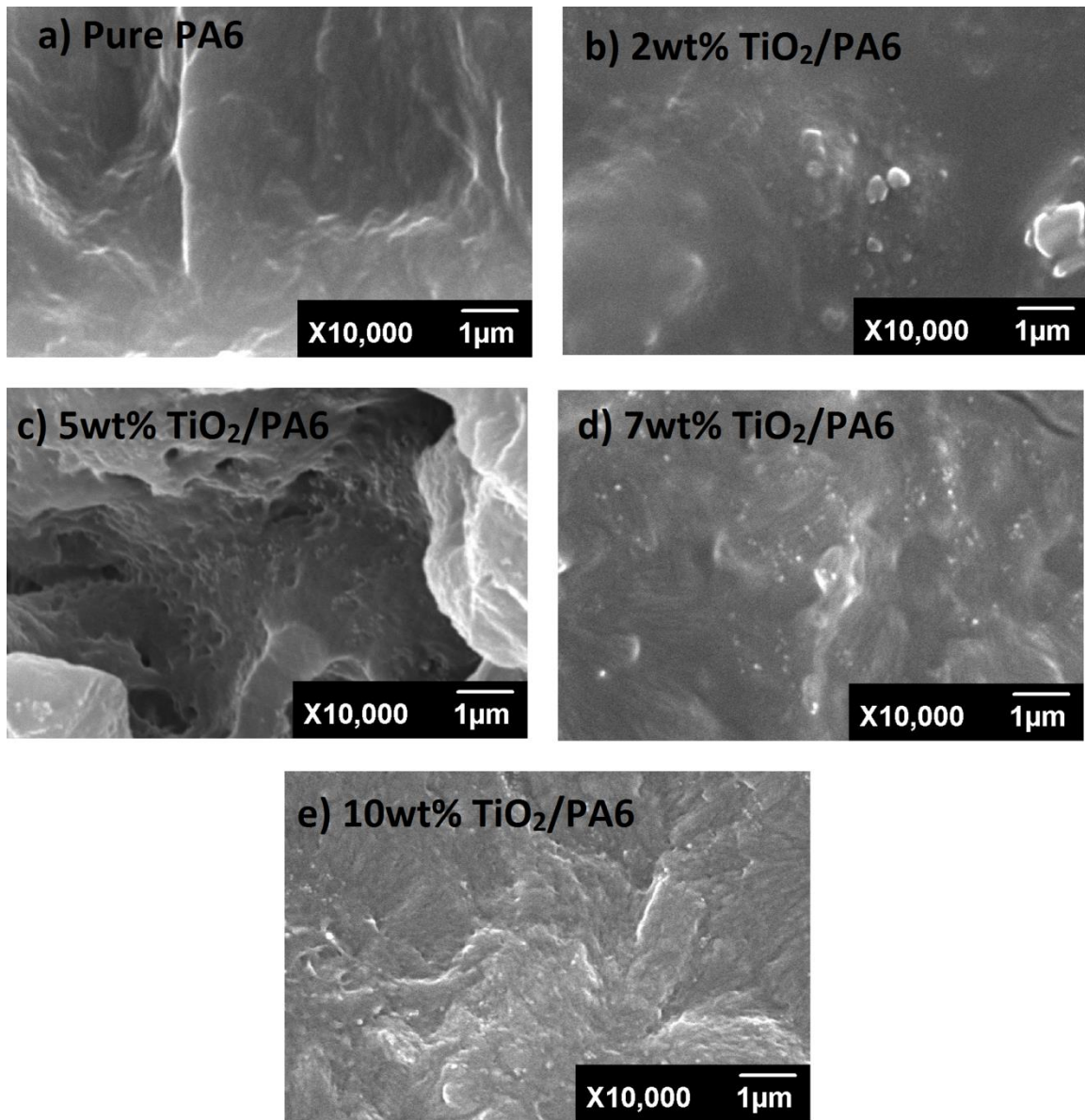


Figure 5.2 Cross sectional SEM images of a. Pure PA6 b. PA6/2wt%- TiO₂ c. PA6/5wt%- TiO₂ d. PA6/7wt%-TiO₂ e. PA6/10wt%-TiO₂

Morphology of the second set of membranes is compared using SEM micrographs of Pure Psf and Psf/TiO₂ at a resolution of x10, 000 for surface and cross section. The SEM analysis revealed that fabricated membranes have dense structure (Figure 5.3). Pure Psf has smooth surface (Figure 5.3a) but Psf/TiO₂ has slightly rough surface as the concentration of nanoparticles are increased. SEM micrograph depicts the presence of

TiO₂ at the surface of MMMs. The cross sectional micrographs (Figure 5.4) demonstrates that in case of pure PSf and PSf/TiO₂ the cross sections are smooth and dense.

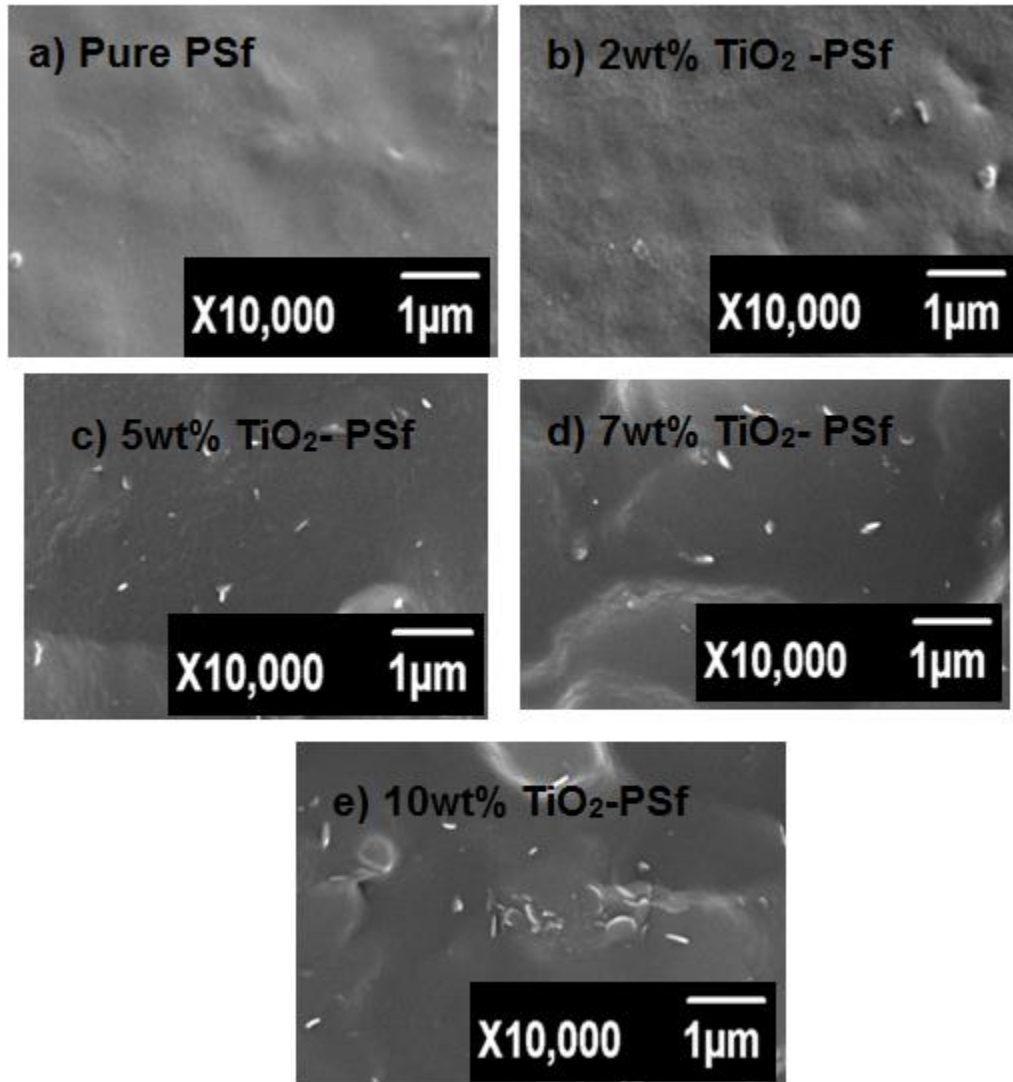


Figure 5.3 Surface Morphology of a. Pure PSf b. PSf /2wt%- TiO₂ c. PSf /5wt%- TiO₂ d. PSf /7wt%- TiO₂ e PSf /10wt%-TiO₂

In the cross sectional micrographs (Figure 5.4) the homogeneity of TiO₂ in 2-10% was observed however micrograph confirms agglomeration in case of 10% TiO₂. Although the interaction in 2% TiO₂ is stronger but the amount of TiO₂ are not enough to give required permeability. In case of 5-10% TiO₂ the homogeneity, optimum amount of TiO₂

and slightly better interaction between TiO_2 and polymer chains results in less void formation at the edges of TiO_2 .

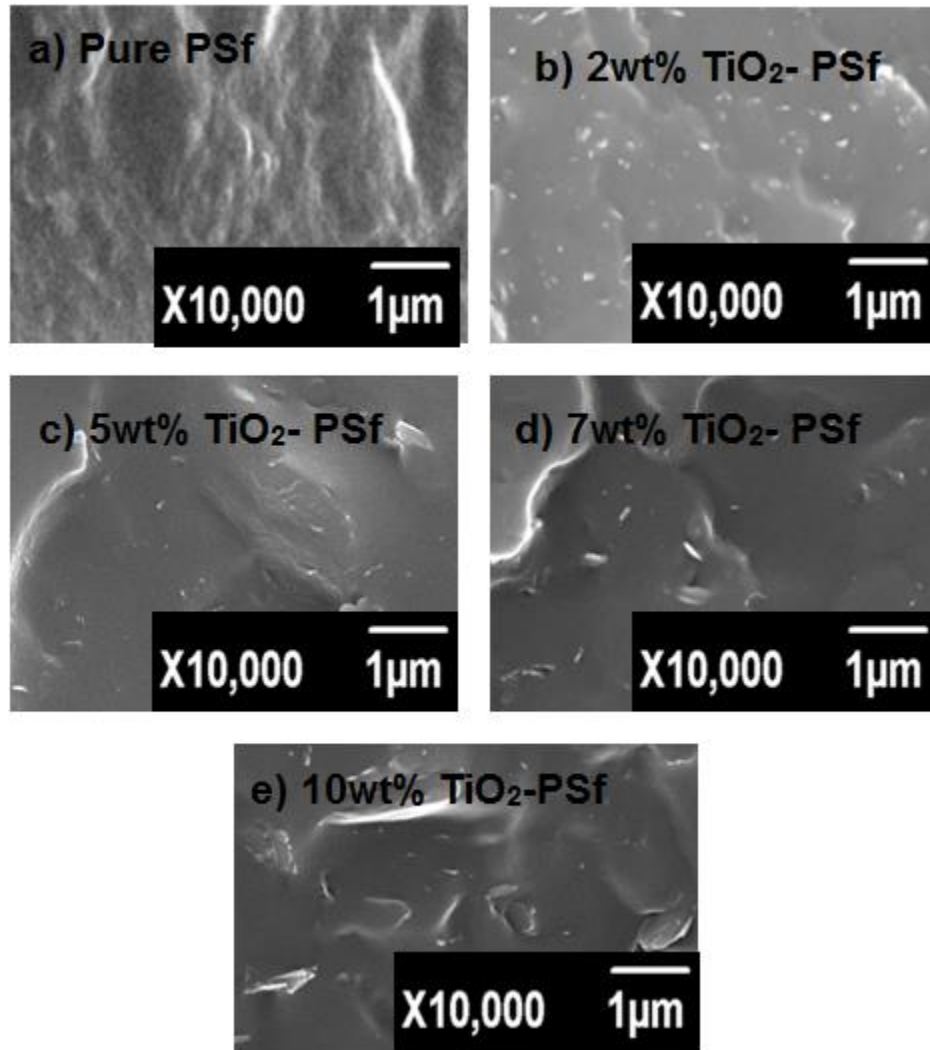


Figure 5.4 Cross sectional SEM images of a. Pure PSf b PSf /2wt%- TiO_2 c. PSf /5wt%- TiO_2 d. PSf /7wt%- TiO_2 e. PSf /10wt%- TiO_2

5.2. Mechanical testing

Figure 5.5 represents the stress strain graph of the fabricated membranes PA6/TiO₂ (0, 2, 5, 7, 10wt %). PA6 containing 2wt% Titania nanoparticles have the maximum tensile strength and percentage elongation. Due to the small size and high surface area of Titania particles it has the ability to make interaction with polymer which tends to enhance the mechanical properties of the polymer. When the Titania nanoparticles load is low, the interaction between the nanoparticles and the polymer is low due to the long distance between them. As the load of Titania nanoparticles are increased the interaction become stronger between the nanopartilces and the polymer. This is due to the shorter distance between them. However, if the concentrations of Titania particles are increased there will be agglomeration which will tend to decrease the mechanical properties of the polymer because the aggregated particles will act as stress concentrators.

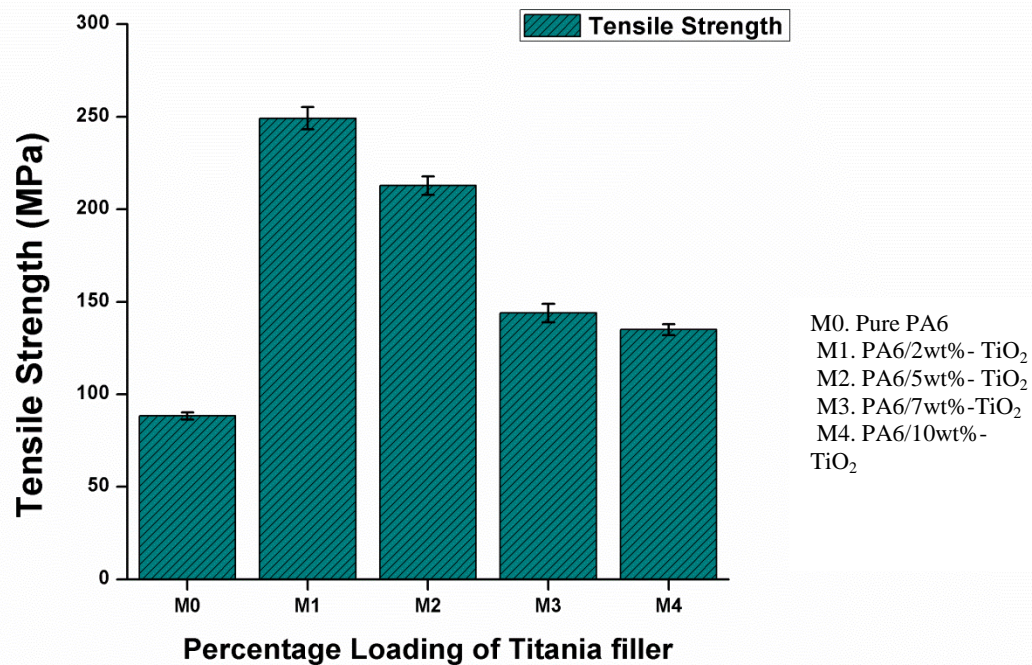


Figure 5.5: Tensile strength bar graph of pure PA6 and PA6/TiO₂ membranes

Figure 5.6 illustrates the trend between the tensile strength and percentage elongation with the pure membrane and fabricated membranes i.e. having different concentrations of nanoparticles TiO₂ (0, 2, 5, 7, 10wt %). There is a sharp decline in the tensile strength from 212.8 MPA to 134.9MPA as the concentration of Titania changes from 5wt% to 10wt%. Similarly, same behavior was seen in the %elongation graph i.e. the decrease from 12.7 to 6.9%. This drop off in the tensile strength and %elongation can be due to the presence of stress concentrators. As we increase the concentration of nanoparticles, it may agglomerate and in turns decrease the mechanical properties. The increase in the wt% of Titania also leads to the voids formation which disturbs the pattern of the polymer chains and increasing the free volume resulting in the decrease of mechanical properties i.e. tensile strength and %elongation.

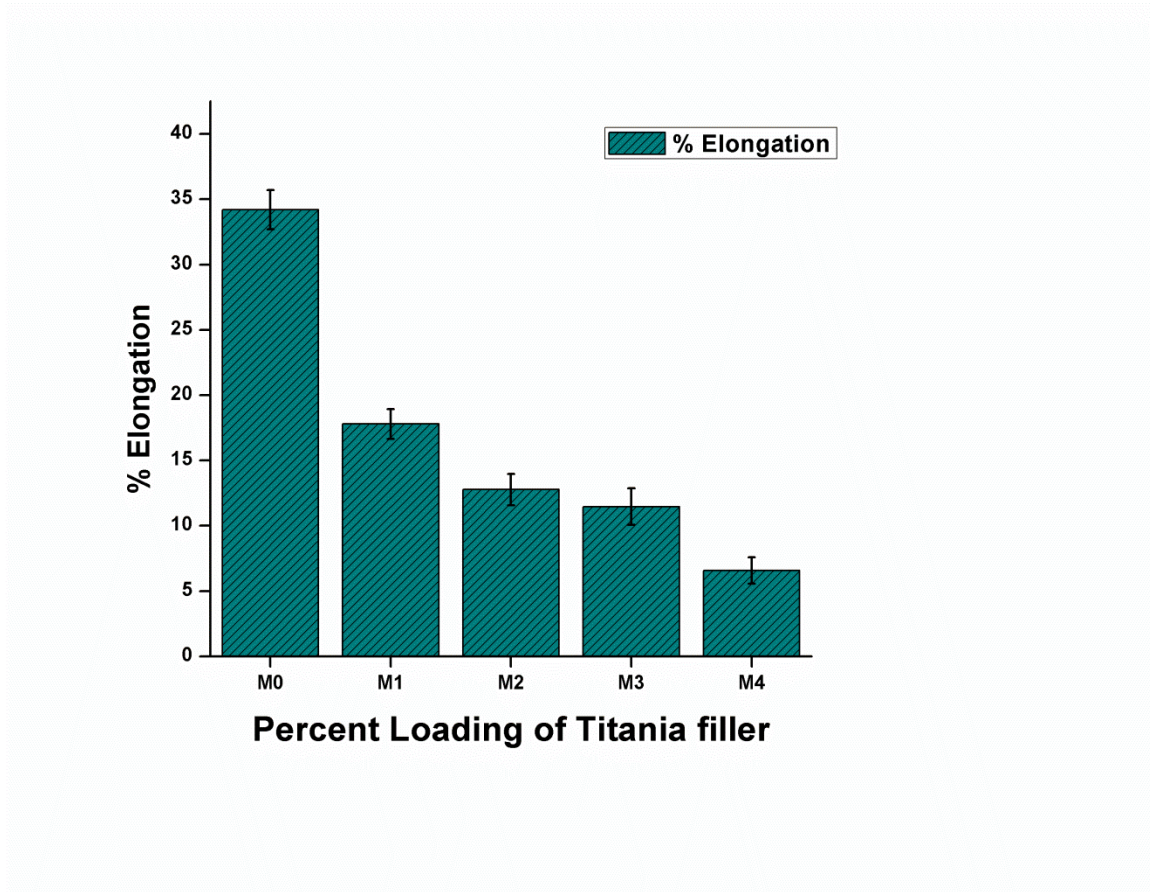


Figure 5.6: % elongation curves as a function of TiO_2 nanoparticles(wt%)

Figure 5.7 shows the stress strain curve of pure polymeric membrane and fabricated nanocomposite membranes containing different concentration of TiO_2 (2, 5, 7, 10 wt. %). Results revealed that fabricated pure polymeric membrane has lower tensile strength than the membranes having nanoparticles. From these results it is concluded that membrane was stiff and brittle.

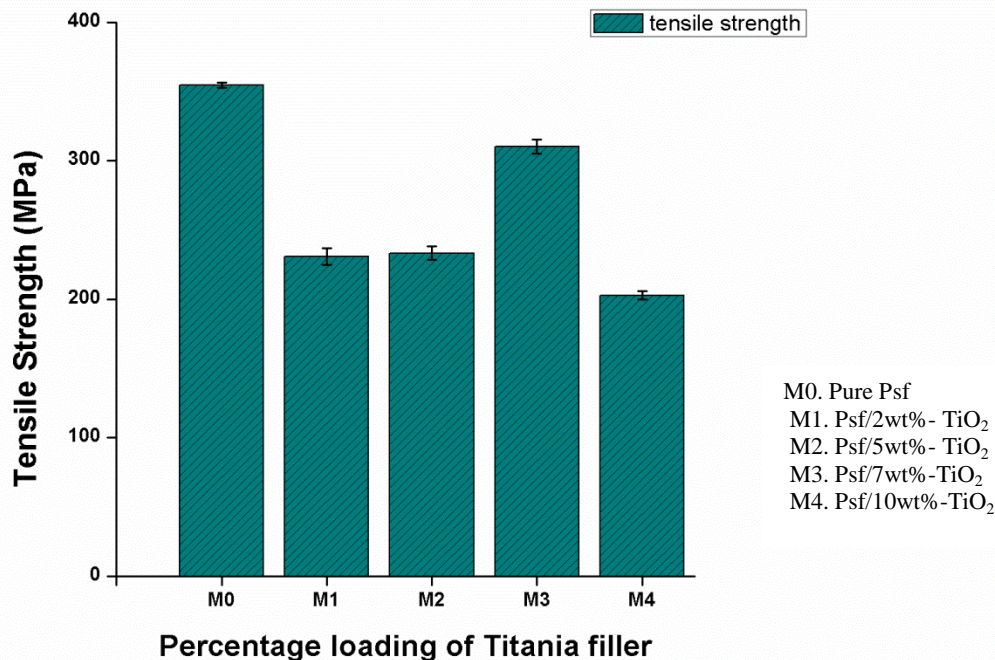


Figure 5.7: Tensile strength bar graph of pure Psf and Psf/TiO₂ membranes

Mechanical testing results showed that by increasing the concentration of TiO₂ up to 10 wt. % results in an increase in tensile strength. Increase in titania nanoparticles concentration from 0 to 5wt. % leads to an improved tensile strength. Percentage elongation was also increased up to 75% by increasing the concentration of titania (0 to 5 wt. %) as shown in figure 5.8. The increased in tensile strength and % elongation is credited to the strong bonding between titania nanoparticles and polymer matrix and homogenous dispersion of TiO₂ as observed by SEM results.

Mechanical properties were decreased as the concentration of TiO₂ was increased till 10 wt. %. % elongation was decreased from 75 % to 68 % and Tensile strength of membranes was decreased by increasing the wt% of Titania from 5 wt % to 10wt. %. The two reasons behind the decrease in tensile strength are as follows.

- Accumulated fillers behave like stress concentrators which have low surface area.
- The interaction between the polymer and TiO_2 results in improved permeability of membranes with TiO_2 . This is due to the disturbance in the packing of polymer chains which will enlarge the voids and free volume which in turn drop off the tensile strength and % elongation.

Decrease in percentage elongation shows brittleness of specimen, which may be due to the restriction in the movement of polymer chains.

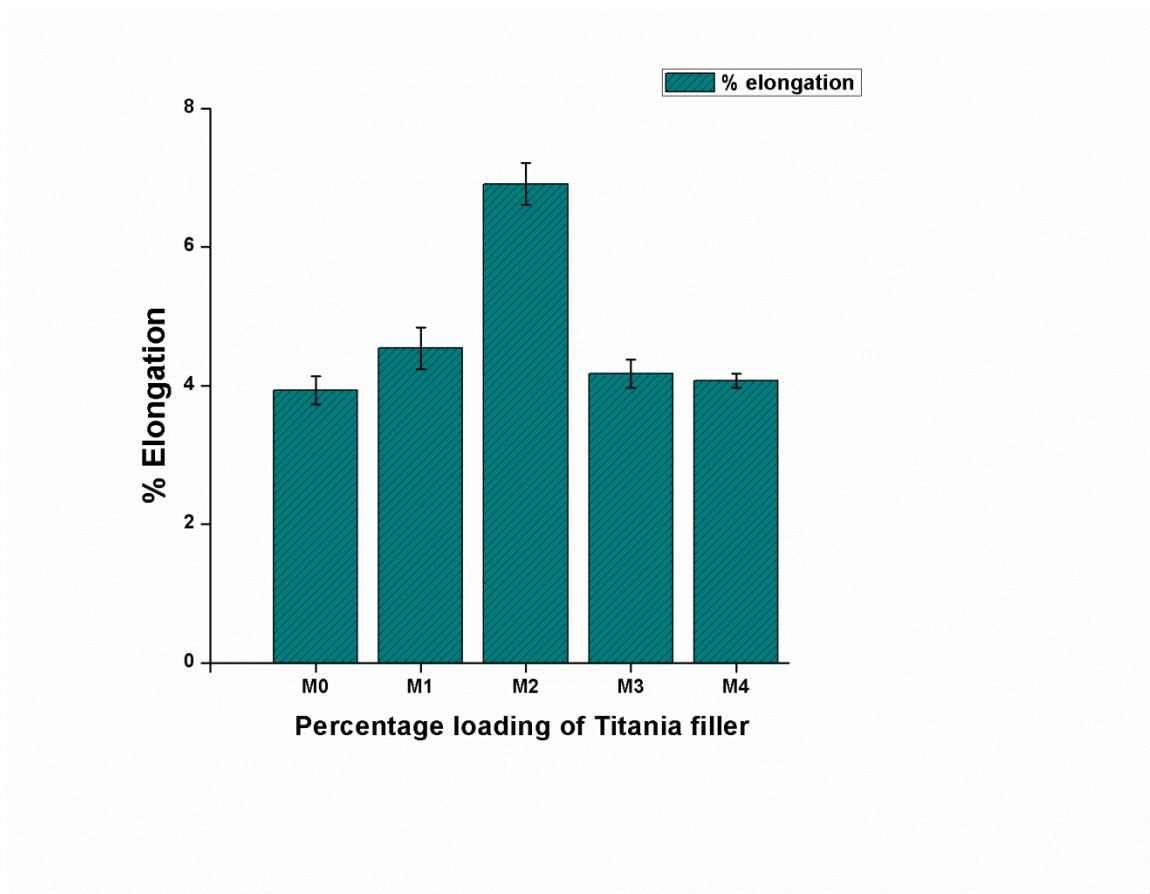


Figure 5.8: % elongation curves as a function of TiO_2 nanoparticles(wt%)

5.3. Thermal Gravimetric Analysis

Diamond TG/DTA Perkin Elmer was used to study the heat treatment of the PA6, and PA6/ TiO_2 , Thermal stability and weight changes were analyzed. 2mg sample in

aluminum pans was used and Nitrogen atmosphere (30-500 °C). Samples were run at 10 °C/min heating rate and 80ml/min gas flow.

The weight loss curve of the pure membrane PA6 is represented in figure 5.9. TGA curve of the PA6 curve shows the decomposition starts around the temperature range of 330-360°C and the final decomposition starts at 500°C.

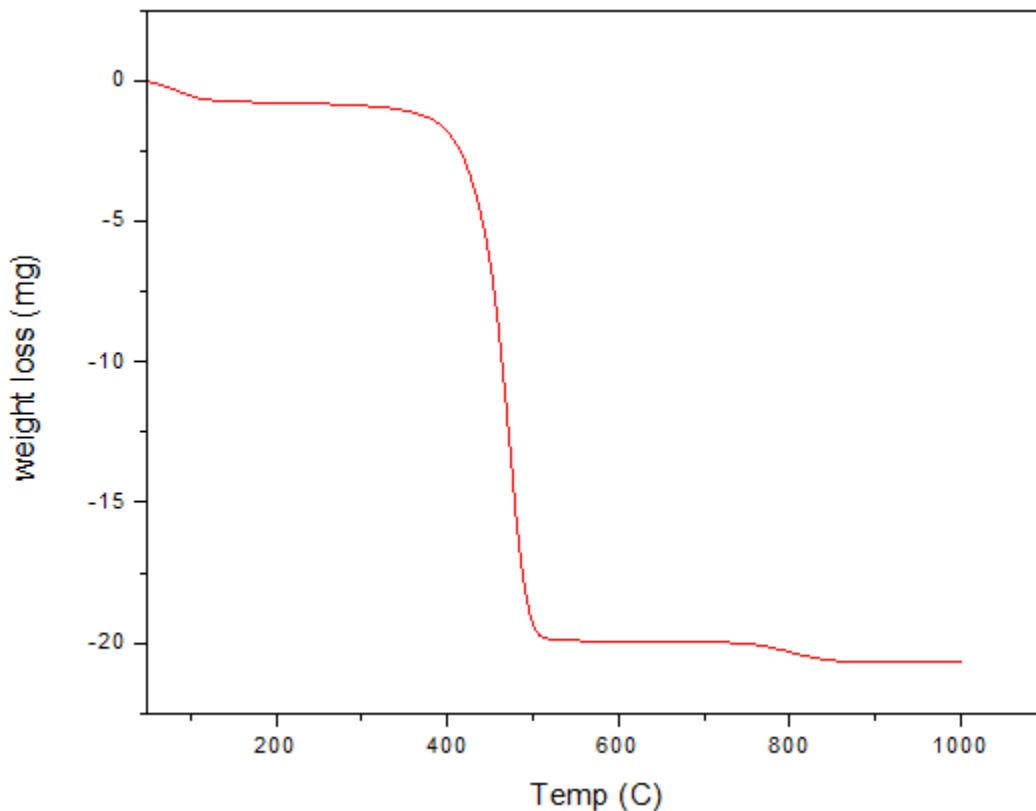


Figure 5.9: TGA curve of pure PA6 membrane

Figure 5.10 shows the weight loss curve of PA6/TiO₂ at varied weight fraction of TiO₂. From the TGA curves it can be observed that residue weight has increased with increasing weight fraction of titania nanoparticles indicating that polymer has totally degraded at around 500 °C and residue contains only titania nanoparticles. TGA results

revealed that all membranes are thermally stable up to 410 °C and after that they begin to degrade and weight become fairly constant at around 500 °C.

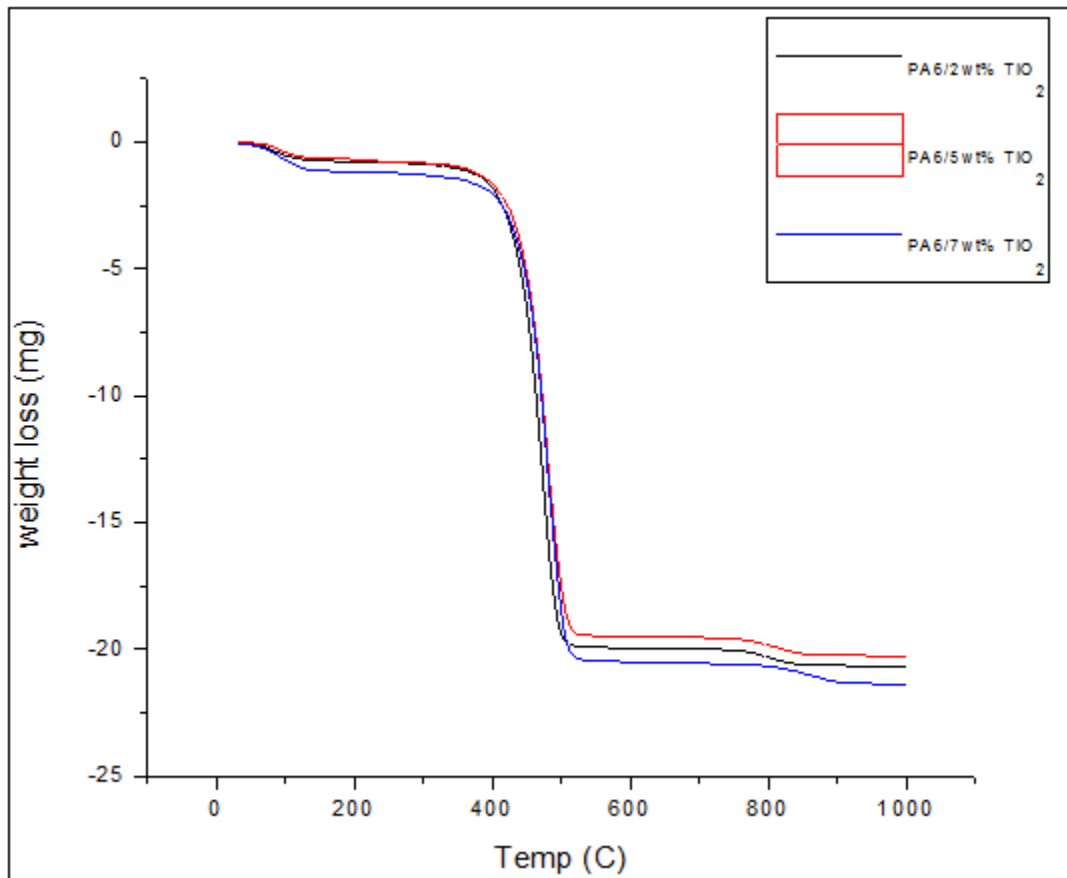


Figure 5.10: TGA Curves of Various Composite membranes

The weight loss curve of the pure membrane Psf is represented in figure 5.11. TGA curve of the Psf curve the decomposition starts around the temperature range of 400-450°C and the final decomposition starts at 500°C. Figure 5.11 shows the weight loss curve of Psf/TiO₂ at varied weight fraction of TiO₂. From the TGA curves it can be observed that

residue weight has increased with increasing weight fraction of titania nanoparticles indicating that polymer has totally degraded at around 500 °C and residue contains only titania nanoparticles. TGA results revealed that all membranes up to 450 °C are thermally stable and after that they begin to degrade and weight become fairly constant at around 540 °C.

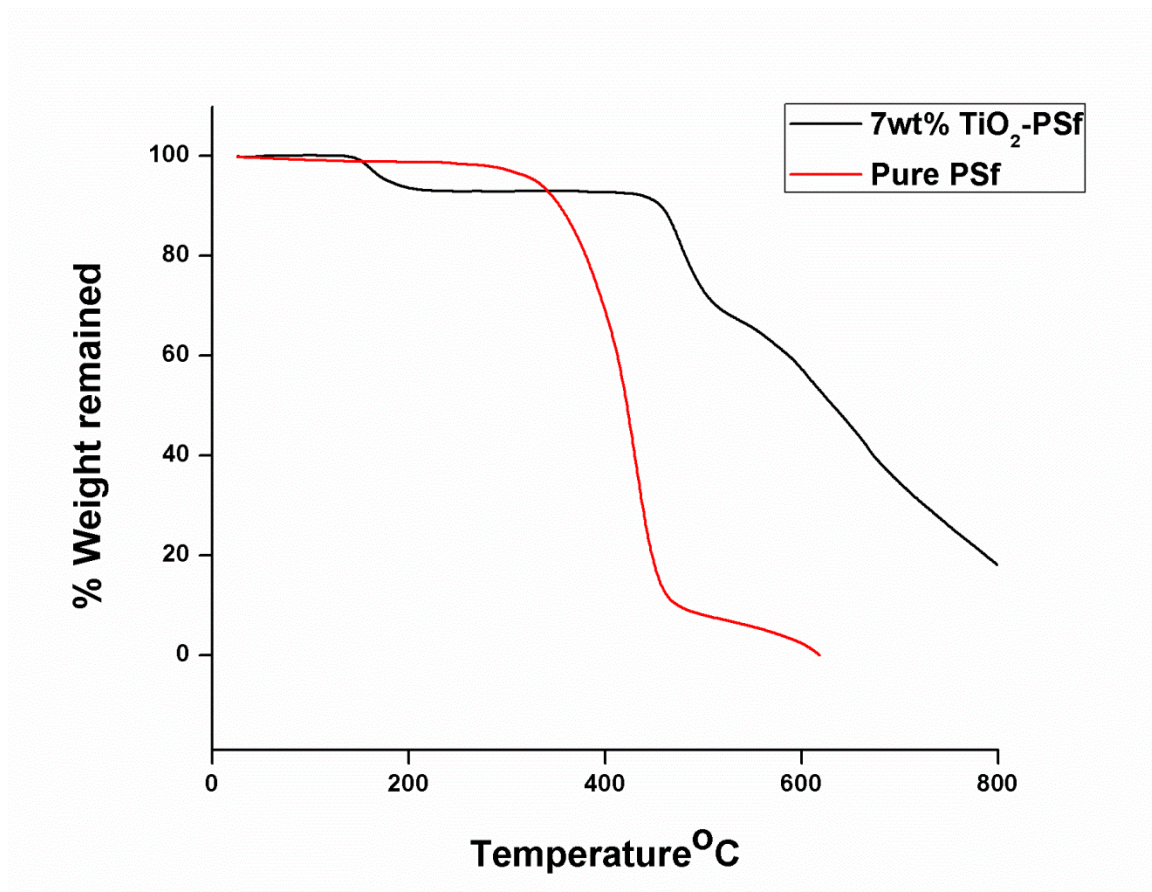


Figure 5.11: TGA Curves of Various Composite membranes

5.4. Gas permeation results

For gas permeation properties, PA6 and PA6/TiO₂ membranes were cut into 8.5 cm² circular shape and placed in the membrane cell. The measurements were taken at

pressures of 2-4 bars at room temperature with dry single gases CO₂, N₂ and O₂. Gas permeating tests were studied in following ways.

- With increasing Loading ratio
- With increasing Feed pressure

Figure 5.12 represents the effect of pressure with permeability. The permeability decreases with the increase in pressure for all the gases CO₂, O₂ and N₂. This is because by increasing the change in pressure the flow rate increases significantly due to which there is a decrease in the permeability value. This can be verified by fick's law. Among all the gases, the decrease in permeability is greater for N₂ followed by O₂ then CO₂. It can be explained through the kinetic diameter of the gases. As the kinetic diameter of N₂ molecules are large compared to other two gases due to which it shows the maximum decrease in permeability among the gases. Contrary to this, CO₂ being polar in nature interact with the NH group of the membrane resulting in the high decrease of the permeability.

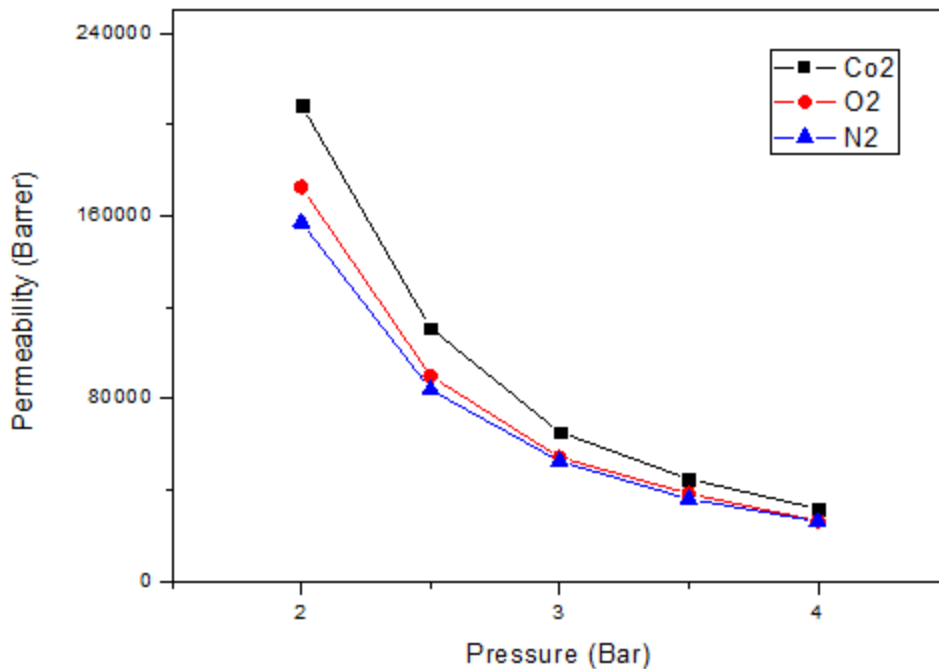


Figure 5.12: Trend of permeability with pressure of PA6

As illustrated in the figure 5.13 the permeability of all the gases increased for Titania loading from 2wt% to 7wt% and then is decreased at 10wt%. According to solution

diffusion mechanism, the gas permeability depends upon on the two factors gas sorption and diffusion. The presence of inorganic filler greatly affects the gas permeation as the interaction between the filler and polymer is improved. So the permeation increases as the filler wt% increases.

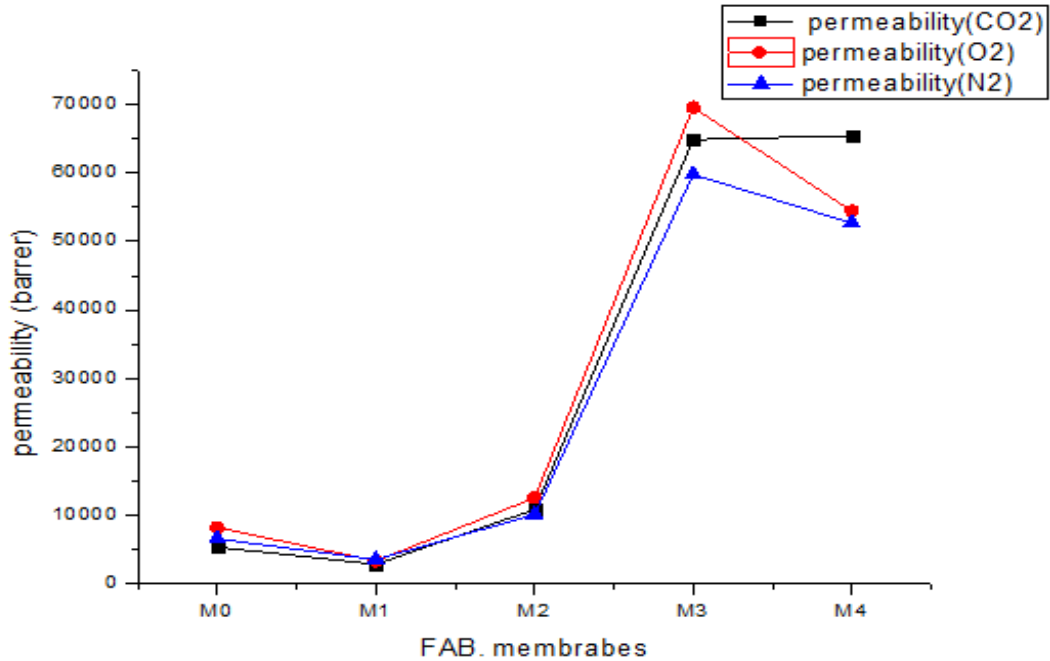


Figure 5.13: TiO₂ loading ratio vs. permeability of PA6 and PA6/TiO₂ membranes

Figure 5.17a, b and c shows the effect of wt% of Titania nanoparticles on the permeability of carbon dioxide, oxygen and nitrogen correspondingly. The result shows that with increasing wt% of TiO₂ bar upto 7wt% at pressure of 3.5 the permeability of these gases was increased. The interaction of the polymer chains with TiO₂ results in improved permeability of membranes with TiO₂. This is due to the disturbance in the polymer chains which will enlarge the voids and so its free volume [38]. The enhanced gas permeability is due to the gas molecules pass through these voids. SEM results shows voids are increased with increasing wt% of TiO₂.

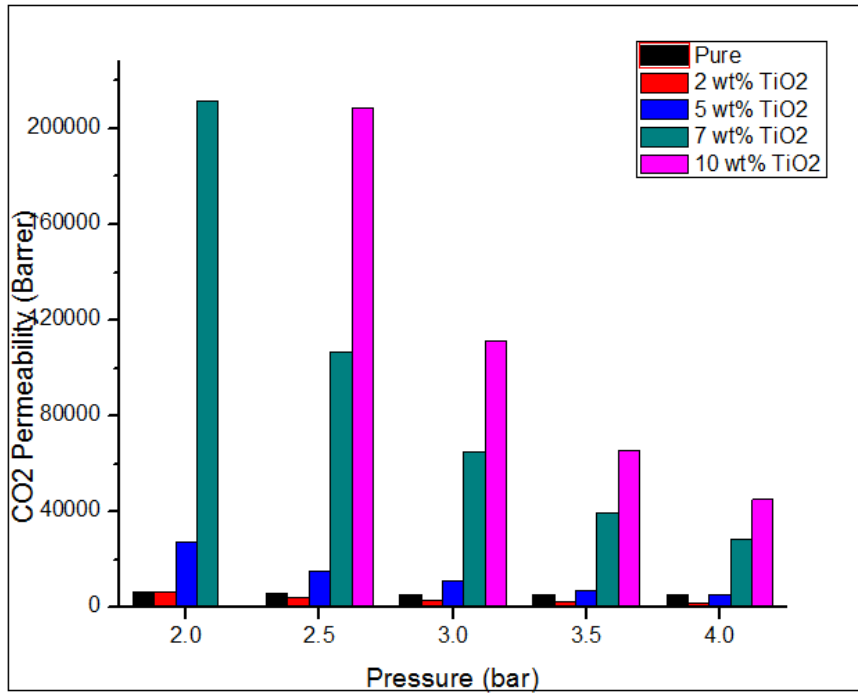


Figure 5.17a: Gas permeability of CO₂ with increasing TiO₂ loading ratio

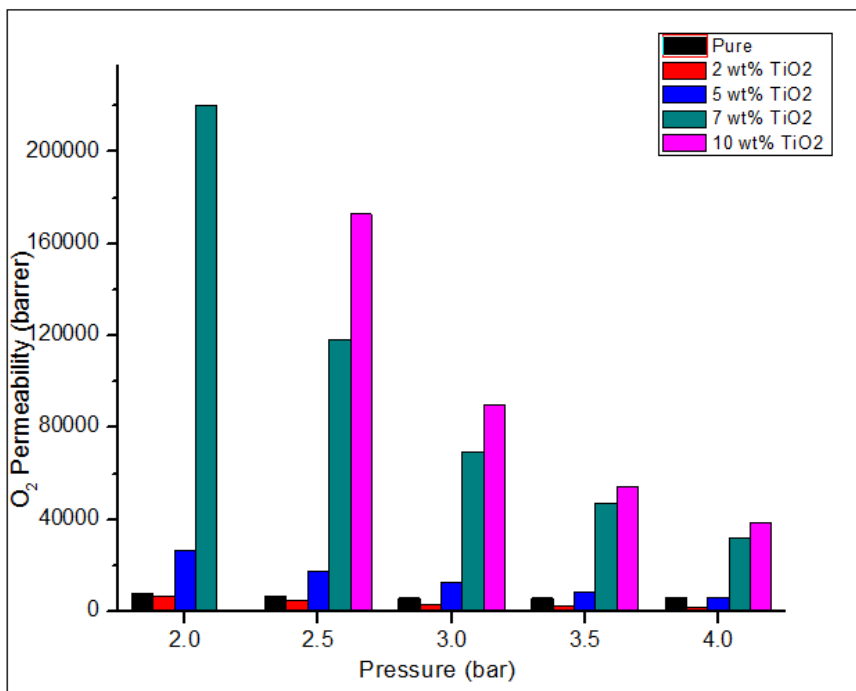


Figure 5.17b: Gas permeability of O₂ with increasing TiO₂ loading ratio

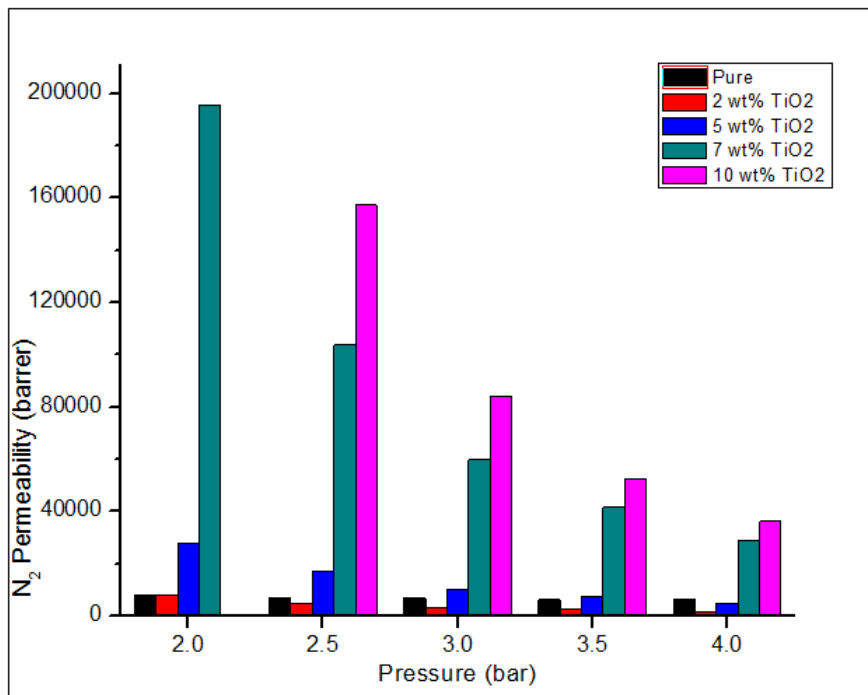


Figure 5.17c: Gas permeability of N₂ with increasing TiO₂ loading ratio

The comparison of permeabilities of carbon dioxide, oxygen and nitrogen with increasing concentration of TiO₂. Results revealed that carbon dioxide has higher permeability than oxygen and nitrogen. High permeability of carbon dioxide is linked with its lower kinetic diameter than other gases (CO₂ (3.3 Å) < O₂ (3.46 Å) < N₂ (3.64 Å)) [38, 39].

Also the inorganic fillers have some unique interaction with the gases like carbon dioxide increases the gas permeability in nanocomposite membranes [40]. Titania nanoparticles were used in this work which justifies the higher permeability of carbon dioxide.

O₂/N₂ and CO₂/N₂ selectivities of composite membranes at pressure of 3 bar are shown in Figure 5.18. Permselectivity of gas pair O₂/N₂ and CO₂/N₂ was around 1 with increasing concentration of TiO₂ till 10 wt. % TiO₂. Highest selectivity ($\alpha_{O_2/N_2} = 1$) was obtained with 2wt. % TiO₂. But on increasing the wt% of TiO₂, selectivity was decreased considerably due to considerable increase in gas permeability.

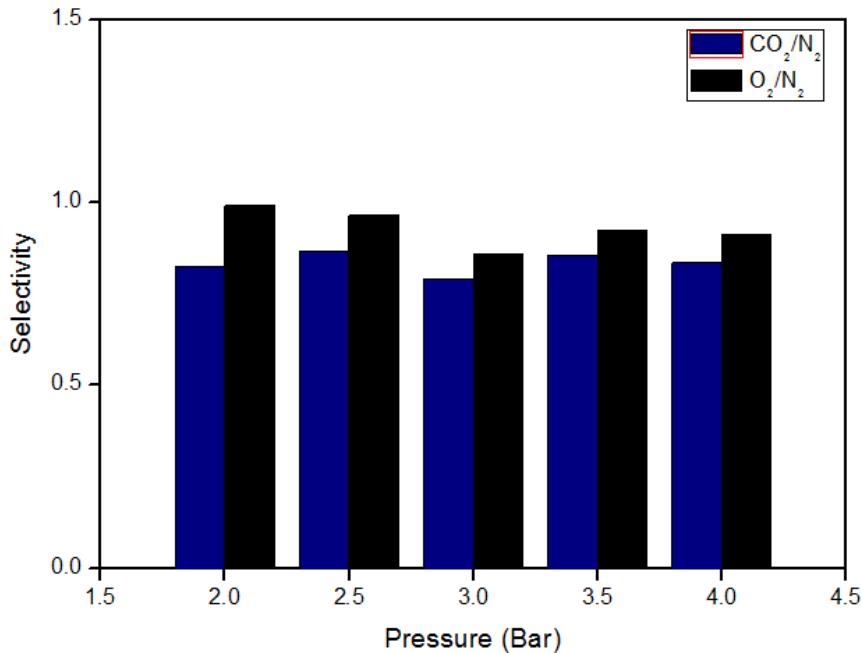


Figure 5.18: Feed Pressure Vs O₂/N₂ and CO₂/N₂ selectivity

The permeability of CO₂, N₂ and O₂ at pressure range 2–4 bar for pure polysulfone membrane is shown in Figure 5.14. As indicated in the fig, CO₂, N₂ and O₂ permeability decreased and reached to a minimum by increasing pressure. Decrease in permeability is observed which depicts that flow of gases through dense membranes is not too much dependent on pressure and there is a very slight increase in the flow rate with pressure and hence permeability decreases as we increase the pressure.

According to Figure 5.15 the change in permeability of CO₂, N₂ and O₂ for pure and modified membranes can be observed. There is a very slight change in permeability of CO₂, N₂ and O₂ for 2, 5, 7 and 10% TiO₂. As per solution diffusion model permeability is inversely related to differential pressure. The decrease in permeability is due to the fact that the flow rate of gas is not increasing as much at higher pressure as it was on the lower pressure.

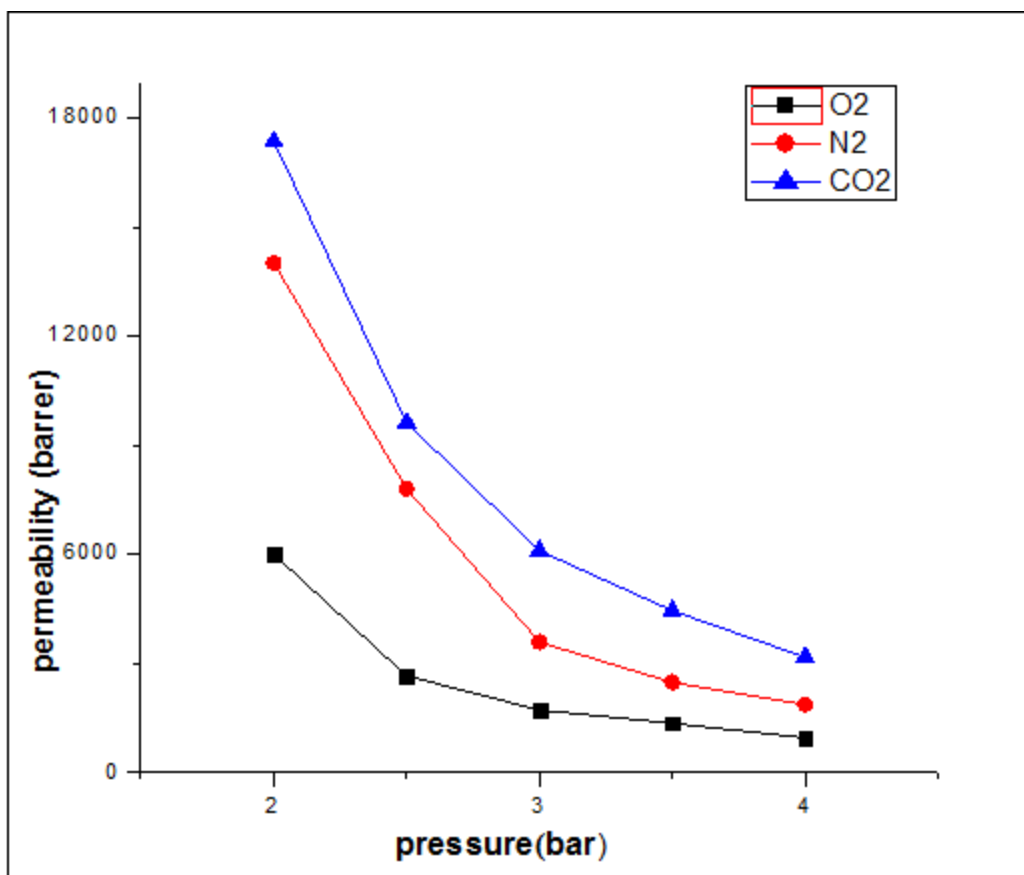


Figure 5.14: Trend of permeability with pressure of Psf

Also the chains are packed and permeability mainly depends upon the interaction of gas molecule with the OH functional group attached to the chains, which in case of CO₂ facilitate its diffusion due to quadrupole moment associated with CO₂. In case of TiO₂ the interaction between TiO₂ and Psf determines the permeability of N₂ and O₂. In case of 5% TiO₂ the interaction between TiO₂ and Psf is weak (Figure 5.15) producing small spaces between TiO₂ and Psf matrix allowing the gas a non-selective path while in case of 7 and 10% TiO₂ the interaction is strong and the permeability is either through the TiO₂ or due to movement of chains which hinders the movement of N₂ and O₂ molecules and allow CO₂ to pass preferably.

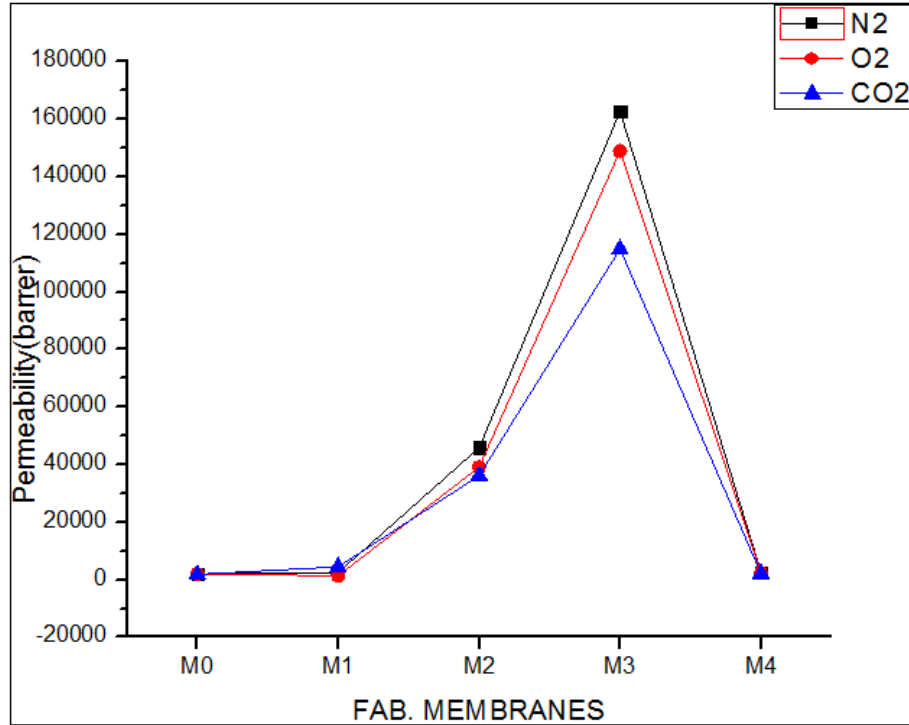


Figure 5.15: Trend of Permeability of Psf and Psf/TiO₂ membranes with different TiO₂ contents

Presence of TiO₂ decreases the permeability compared to pure Psf membrane which is in accordance with Maxwell model. According to this model diffusion of a gas through membrane decreases with the addition of a filler [26]. Effect of filler weight percentage on permeability and CO₂/N₂ and O₂/N₂ selectivity is shown in Figure 5.16 a, b, c and d.

Figure 5.17 demonstrates a slight decrease in permeability in most cases except 10% TiO₂ which depicts that flow of gases through dense membranes is not too much dependent on pressure and there is a very slight increase in the flow rate with pressure and hence permeability decreases as we increase the pressure while 10% TiO₂ does not behave like other membranes due to poor interaction of TiO₂ with the polymer caused by agglomeration.

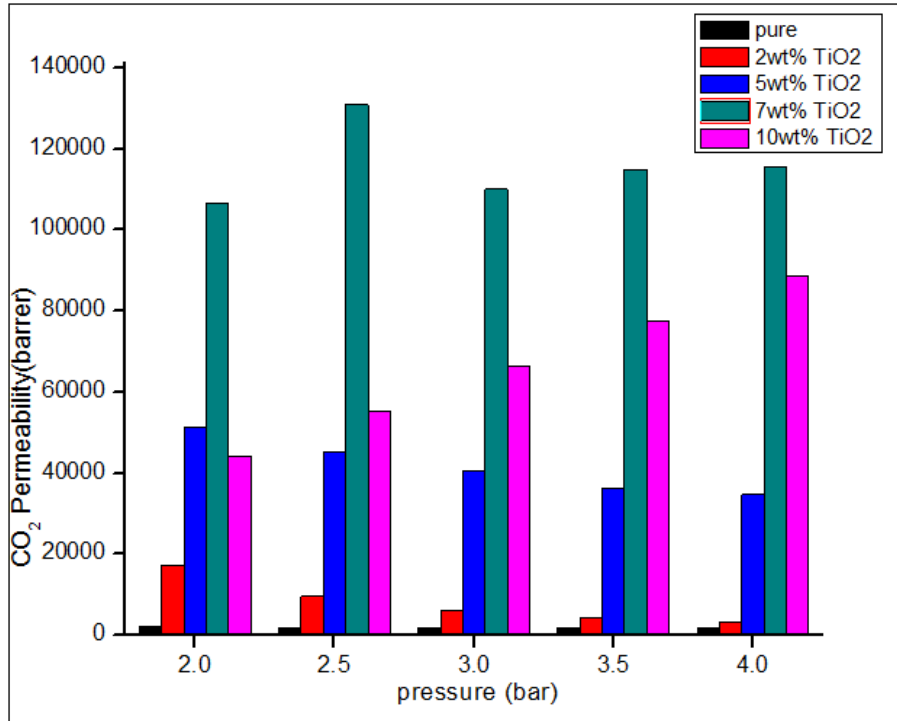


Figure 5.16a: Gas permeability of CO₂ with increasing TiO₂ loading ratio

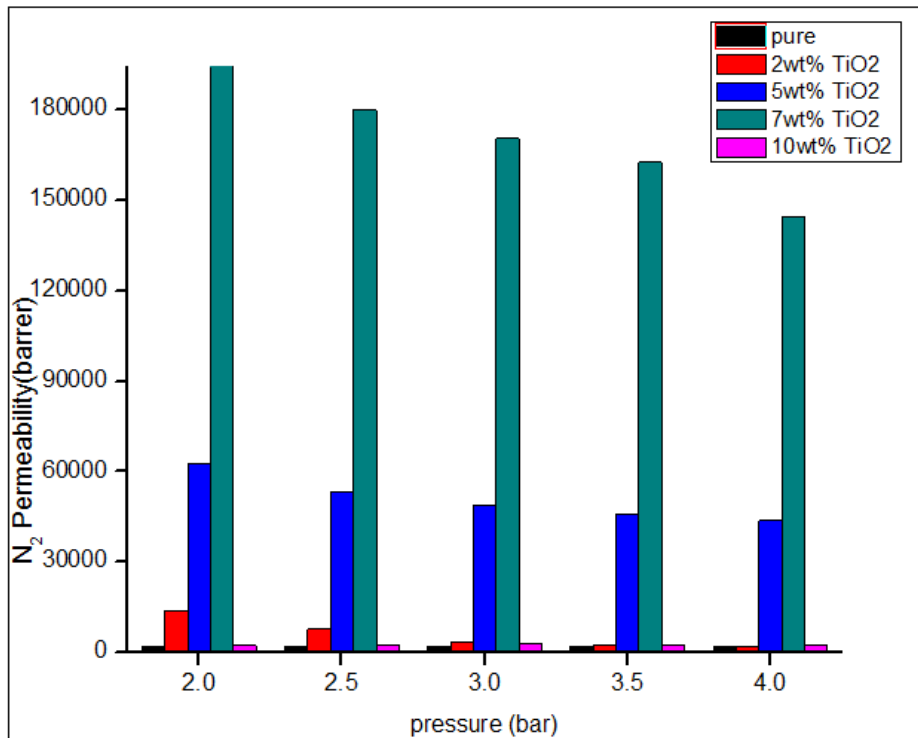


Figure 5.16b: Gas permeability of N₂ with increasing TiO₂ loading ratio

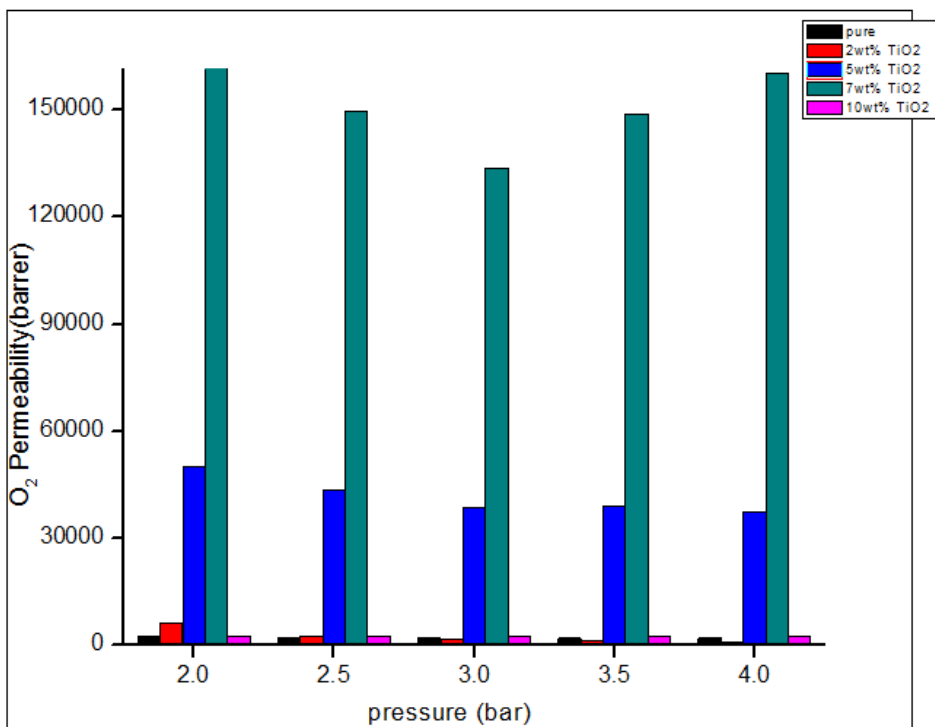


Figure 5.16c: Gas permeability of O₂ with increasing TiO₂ loading ratio

Permselectivity of O₂/N₂ and CO₂/N₂ gas pairs were investigated with increasing wt% of Titania nanoparticles (0, 2, 5, 7 and 10%) as shown in figure 5.16d. It was observed that O₂/N₂ and CO₂/N₂ selectivity was higher at 2 wt% Titania and their selectivities decreases as the amount of nanofiller increases. Enhanced permeabilities with 2 wt. % TiO₂ loading at 3.5 bar pressure were obtained due to good interaction between the polymer and nanoparticles which is also confirmed by SEM whereas other wt ratios were least selective due to poor interaction between Titania and polysulfone.

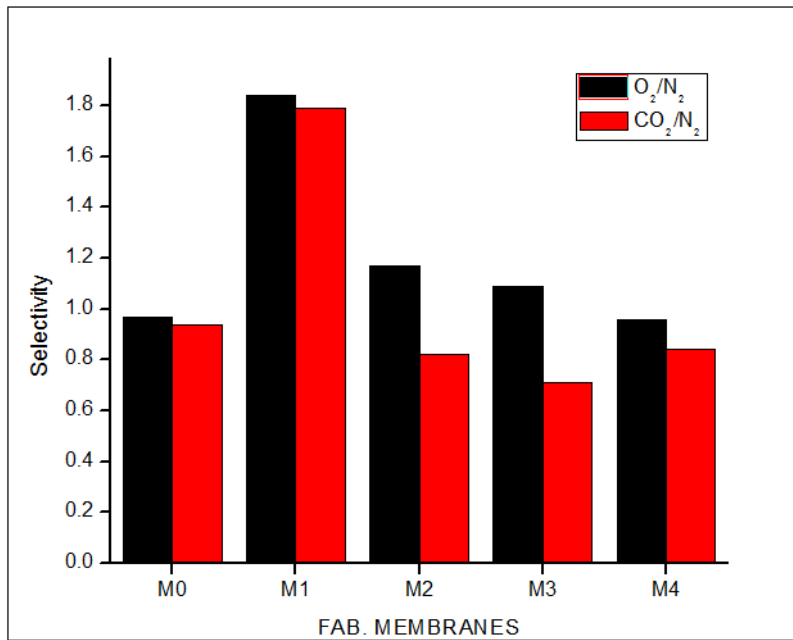


Figure 5.16d: Feed Pressure Vs O₂/N₂ and CO₂/N₂ selectivity

Chapter-6

Conclusions and Recommendations

An overview of the entire research work and the future recommendations are included in this section

6.1. Conclusions

In this study PA6/TiO₂ and Psf/TiO₂ composite membranes were prepared with different TiO₂ loading (0, 2, 5, 7, 10 wt %). Two polymers were chosen for the reason that its excellent toughness, elevated potential flux and superior thermal stability. As a result, by using these polymers blend we can make a good quality merge of glassy polymer and nanoparticles.

The fabricated membranes were characterized with analytical techniques, including scanning electron microscopy (SEM), Universal tensile testing machine (UTM), and thermal gravimetric (TG) analysis. Permeability experiments were performed using CO₂, O₂ and N₂ to check the interaction of TiO₂ with these gases.

Characterization of the fabricated membranes shows that TiO₂ are very companionable with polyamide6 and polysulfone. The gas permeation results shows that permeability of CO₂ was prominent compared to nitrogen and oxygen. Better results in terms of permeability were obtained with 7 wt. % TiO₂ loading.

So, it can be concluded that PA6/TiO₂ and Psf/TiO₂ composite membranes have immense prospective for the permeation of CO₂, O₂ and N₂. As PA6 membranes shows higher permeability so these can be used support layer in the composite membranes where as the Psf membranes are a good option as a active layer in the composite membranes which will shows potential applications in process industries.

6.2. Future Recommendation

TiO₂ nanoparticles which are blended with the polymers polyamide6 and polysulfone can be modified further for gas separation applications. Other than this, the permeability study of other gases such as CH₄ and H₂ can also be done via fabricated blended membranes. Moreover, blend of PA6 and Psf polymers can also be used to enhance permeability of various gases and selectivity can also be studied. Different fillers can also be used to enhance the permeability and selectivity of range of gas pairs in these polymers.

References

1. K. Nath, *Membrane separation processes*
2. J. K. Mitchell, "On the penetrativeness of fluids," *Journal of medical sciences*, 1830.
3. W.J. Koros and G. K. Fleming, "Membrane-based gas separation," *Journal of membrane science*, 1993.
4. M. Mulder, *Basic principles of membrane technology*: Kluwer Academic Publishers, 1996.
5. R. W. Baker, *Membrane Technology and Applications*, 2003.
6. Nunes and S. P. Peinemann, "Membrane materials and membrane preparation in membrane technology in the chemical industry," 2001.
7. D. Gomes, S. P. Nunes, and K. V. Peinemann, "Membranes for gas separation based on poly(1-trimethylsilyl-1-propyne)–silica nanocomposites," vol. 246, pp. 13-25, 2005.
8. R. Z. Raymond and G. K. Fleming, *Gas permeation in Membrane Handbook*. New York, 1992.
9. Baker, *Future directions of membrane gas separation technology*, 2002.
10. P. Pandey and R. S. Chauhan, "Membranes for gas separation," *Prog. Polym. Sci.*, vol. 26, no. 6, pp. 853–893, 2001.
11. K. Scott, *Membrane separation technology*: Scientific & Technical Information, 1990.
12. S. K. Sen and S. Banerjee, *Journal of membrane sciences*, p. 350, 2010.
13. W. Albrecht, K. Kneifel, T. Weigel, R. Hilke, R. Just, M. Schossig, *et al.*, *J. Membr. Sci*, p. 262, 2005.
14. S. Sridhar, R. Suryamurali, B. Smitha, and T. M. Aminabhavi, *Colloids Surf. A: Physicochem. Eng.*, p. 297, 2007.
15. D. M. Muñoz, E. M. May, J. d. Abajo, J. G. d. I. Campa, and A. E. Lozano, *J. Membr. Sci*, p. 323, 2008.
16. L. M. Robeson, *J. Membr. Sci*, p. 320, 2008.

17. N. P. Patel, C. M. Aberg, A. M. Sanchez, M. D. Capracotta, J. D. Martin, and R. J. Spontak, "Morphological, mechanical and gas-transport characteristics of crosslinked poly(propylene glycol), homopolymers, nanocomposites and blends," *Polymer*, 2004.
18. S. Kazama and M. Sakashita, "Gas separation properties and morphology of asymmetric hollow fiber membranes made from cardo polyamide," *J. Memb. Sci.*, vol. 243, no. 1–2, pp. 59–68, 2004.
19. I. Genne, S. Kuypers, and R. Leysen, "Effect of the addition of ZrO₂ to polysulfone based UF membranes," *Journal of membrane sciences*, pp. 343-350, 1996.
20. N. M. Wara, L. F. Francis, and B. V. Velamakanni, "Addition of alumina to cellulose acetate membranes," *Journal of membrane sciences*, pp. 43-49, 1995.
21. G. Maier, "Gas Separation with Polymer Membranes," *Angew. Chemie Int. Ed.*, vol. 37, no. 21, pp. 2960–2974, 1998.
22. Q.-Y. Wu, L.-S. Wan, and Z.-K. Xu, "Structure and performance of polyacrylonitrile membranes prepared via thermally induced phase separation," *J. Memb. Sci.*, vol. 409–410, no. 5, pp. 355–364, 2012.
23. "High-performance aromatic polyamides," *Prog. Polym. Sci.*, vol. 35, no. 5, pp. 623–686, May 2010.
24. A. T. Mohammadi, T. Matsuura, and S. Sourirajan, "Gas separation by silicone-coated dry asymmetric aromatic polyamide membranes," *Gas Sep. Purif.*, vol. 9, no. 3, pp. 181–187, 1995.
25. P. Safaei, A. Marjani, and M. Salimi, "Mixed Matrix Membranes Prepared from High Impact Polystyrene with Dispersed TiO₂ Nanoparticles for Gas Separation," *J. nanostructure*, vol. 6, no. 1, pp. 74–79, 2016.
26. M. Iwata, T. Adachi, M. Tomidokoro, and M. Ohta, "Hybrid sol–gel membranes of polyacrylonitrile–tetraethoxysilane composites for gas permselectivity," *Journal of applied polymer sciences*, vol. 88, 2003.
27. R. Sengupta *et al.*, "A Short Review on Rubber / Clay Nanocomposites With Emphasis on Mechanical Properties," *Engineering*, vol. 47, pp. 21–25, 2007.
28. J. Ahmad, K. Deshmukh, and M. B. Hägg, "Influence of TiO₂ on the Chemical, Mechanical, and Gas Separation Properties of Polyvinyl Alcohol-Titanium Dioxide (PVA-TiO₂) Nanocomposite Membranes," *Int. J. Polym. Anal. Charact.*, vol. 18, no.

- 4, pp. 287–296, 2013.
29. Q. Hu, E. Marand, S. Dhingra, D. Fritsch, and J. Wen, "Poly (amide-imide)/ TiO₂ nano-composite gas separation membranes " Fabrication and characterization," *J. Memb. Sci.*, vol. 135, no. 1, pp. 65–79, 1997.
 30. F. Moghadam, M. R. Omidkhah, E. Vasheghani-Farahani, M. Z. Pedram, and F. Dorosti, "The effect of TiO₂ nanoparticles on gas transport properties of Matrimid5218-based mixed matrix membranes," *Sep. Purif. Technol.*, vol. 77, no. 1, pp. 128–136, 2011.
 31. C. Joly, S. Goizet, J. C. Schrotter, J. Sanchez, and M. Escoubes, "Sol–gel polyimide-silica composite membrane: gas transport properties," *journal of membrane sciences*, pp. 63–74., 1997.
 32. K. Kusakabe, K. Ichiki, J. Hayashi, H. Maeda, and S. Morooka, "Preparation and characterization of silica–polyimide composite membranes coated on porous tubes for CO₂ separation," *Journal of membrane sciences*, pp. 65–75, 1996.
 33. M. Smaïhi, J. C. Schrotter, C. Lesimple, I. Prevost, and C. Guizard, "Gas separation properties of hybrid imide-siloxane copolymers with various silica contents," *Journal of membrane sciences*, pp. 157-170, 2000.
 34. M. Moaddeb and W. J. Koros, "Gas transport properties of thin polymeric membranes in the presence of silicon dioxide particles," *Journal of membrane sciences*, pp. 143–163, 1997.
 35. C. Hibshman, C. J. Cornelius, E. Marand, and J. M. S. , "The gas separation effects of annealing polyimide-organosilicate hybrid membranes," *Journal of membrane sciences*, pp. 25–40, 2003.
 36. T. Suzuki and Y. Yamada, "Physical and gas transport properties of novel hyperbranched polyimide-silica hybrid membranes," *Journal of applied polymer sciences*, pp. 139–146, 2005.
 37. Q. Hu, E. Marand, S. Dhingra, D. Fritsch, J. Wen, and G. Wilkes, "Poly(amideimide)/TiO₂ nano-composite gas separation membranes: fabrication and characterization," *Journal of membrane sciences*, pp. 65-79, 1997.

38. Y. Kong, H. Du, J. Yang, D. Shi, Y. Wang, Y. Zhang, *et al.*, "Study on polyimide/TiO₂ nanocomposite membranes for gas separation," *Desalination*, pp. 49–55, 2002.
39. J. H. Kim and Y. M. Lee, "Gas permeation properties of poly(amide-6-b-ethylene oxide)-silica hybrid membranes," *Journal of membrane sciences*, pp. 209–225, 2001.
40. A. Higuchi, T. Agatsuma, S. Uemiya, T. Kojima, K. Mizoguchi, I. Pinnau, *et al.*, "Preparation and gas permeation of immobilized fullerene membranes," *Journal of applied polymer sciences*, pp. 529–537, 2000.
41. Z. He, I. Pinnau, and A. Morisato, "Nanostructured poly(4-methy-2-pentyne)/silica hybrid membranes for gas separation," *Desalination*, pp. 11–15, 2002.
42. T. C. Merkel, B. D. Freeman, R. J. Spontak, Z. He, I. Pinnau, P. Meakin, *et al.*, "Sorption, transport and structural evidence for enhanced free volume in poly(4-methyl-2-pentyne)/fumed silica nanocomposite membranes," *Chemistry material*, pp. 109-123, 2003.
43. Gurdeep R. Chatwal, Sham K. Anand, Himalaya Publishing House, 2002. Instrumental method of chemical analysis 5th edition
44. Sharma B.K. Goel Publishing House 'Instrumental method of analysis' pg. 234-237
45. <http://mmrc.caltech.edu/FTIR/FTIRintro.pdf>
46. 2004 ASM International. All Rights Reserved. Tensile Testing, Second Edition (#05106G)